Natural Resources Canada | Ressources naturelles Canada

GEOLOGICAL SURVEY OF CANADA
OPEN FILE 8234

Bedrock geochemistry of the central Thelon tectonic zone, Nunavut

J.B. Whalen, R.G. Berman, W.J. Davis, M. Sanborn-Barrie, and L. Nadeau

2018

Celebrating 175 yrs

Canada

GEOLOGICAL SURVEY OF CANADA
OPEN FILE 8234

Bedrock geochemistry of the central Thelon tectonic zone, Nunavut

J.B. Whalen, R.G. Berman, W.J. Davis, M. Sanborn-Barrie, and L. Nadeau

[1] Geological Survey of Canada, 601 Booth Street, Ottawa, Ontario K1A 0E9
[2] Ressources Naturelles Canada, 490 Rue de la Couronne, Québec, Quebec G1K 9A9

2018

Permanent link: https://doi.org/10.4095/306385

This publication is available for free download through GEOSCAN (http://geoscan.nrcan.gc.ca/).

Recommended citation
Whalen, J.B., Berman, R.G., Davis, W.J., Sanborn-Barrie, M., and Nadeau, L., 2018. Bedrock geochemistry of the Thelon tectonic zone, Nunavut; Geological Survey of Canada, Open File 8234, 1 zip file. https://doi.org/10.4095/306385

Table of Contents

Introduction

The Thelon tectonic zone (TTZ) and Taltson magmatic zone (TMZ) comprise a series of pronounced, N- to NNE-striking, magnetic anomalies extending for over 1000 km along the western boundary of the Rae craton from the Arctic Islands to the Alberta Basin (Fig. 1). The tectonic setting of this major orogenic belt is controversial. Hoffman (1988) postulated that the TTZ-TMZ plutonic suites, long considered correlative, represented a ca. 2.0 Ga continental arc built on the western flank of the Rae craton and subsequently intensely deformed during collision with the Slave craton (TTZ) and Buffalo Head terrane (TMZ). Subsequent geological mapping and metamorphic analysis led Thompson (1989) to conclude that the TTZ formed in an intracontinental setting after a period of crustal thinning. Moreover, Chacko et al. (2000) and De et al. (2000) interpreted whole rock geochemical and oxygen isotopic data from the TMZ as supporting interior mountain belt plutonism within an intracontinental setting, far removed from the active plate boundary. This intracontinental model was suggested by Schultz et al. (2007) to apply to the TTZ, based on the limited extent of 2.0 – 1.9 Ga reworking documented in the Queen Maud block, which Hoffman (1988) proposed as an analog to the Tibetan plateau in the Himalayan orogen.

This contribution presents the first large geochemical dataset for TTZ plutonic rocks that includes modern inductively coupled plasma mass spectroscopy (ICPMS) trace element data. These data are critical both for defining the aerial distribution of lithological variations within this plutonic-dominated region, and for interpreting the tectonic setting of plutonism in the TTZ. Additionally, we compare these data from the central TTZ to published geochemical datasets from the TMZ in order to assess potential along-strike differences in plutonic rock geochemistry and what this may mean for tectonic boundary conditions within the Taltson-Thelon corridor.

Geology of the central Thelon Tectonic Zone

This study of the TTZ is based on an initial ten days of helicopter sampling in 2012, followed by seven weeks of targeted bedrock mapping and supporting multidisciplinary studies spanning two field seasons in 2014 and 2016. Work was carried out within 1:250,000 scale NTS map sheets 76H and 76I, which encompass the eastern Slave craton, central TTZ and the western Rae craton between latitudes 65°N and 67°N (Figs. 2; Berman et al., 2015a, b, 2016). Earlier geological investigations include reconnaissance helicopter-grid mapping across the region (Fraser, 1964), and 1:250 000 scale mapping of the western half of the area (Frith, 1982; Thompson, 1986). Frith (1982) interpreted widespread granitoid migmatite in the southern sheet (76H) as part of Slave craton (i.e., Archean age), although a highly magnetic Proterozoic plutonic suite was later established (Frith and van Breemen, 1990). In the northern sheet (76I), Thompson (1986) distinguished migmatite of supracrustal origin from granitoid migmatite, mapped a wide orthopyroxene zone (igneous and/or metamorphic), and allowed that migmatite within the orthopyroxene zone could be Proterozoic in age. Below we summarize the key geological components in these two map sheets (Fig. 2) based on interpretation of all geological

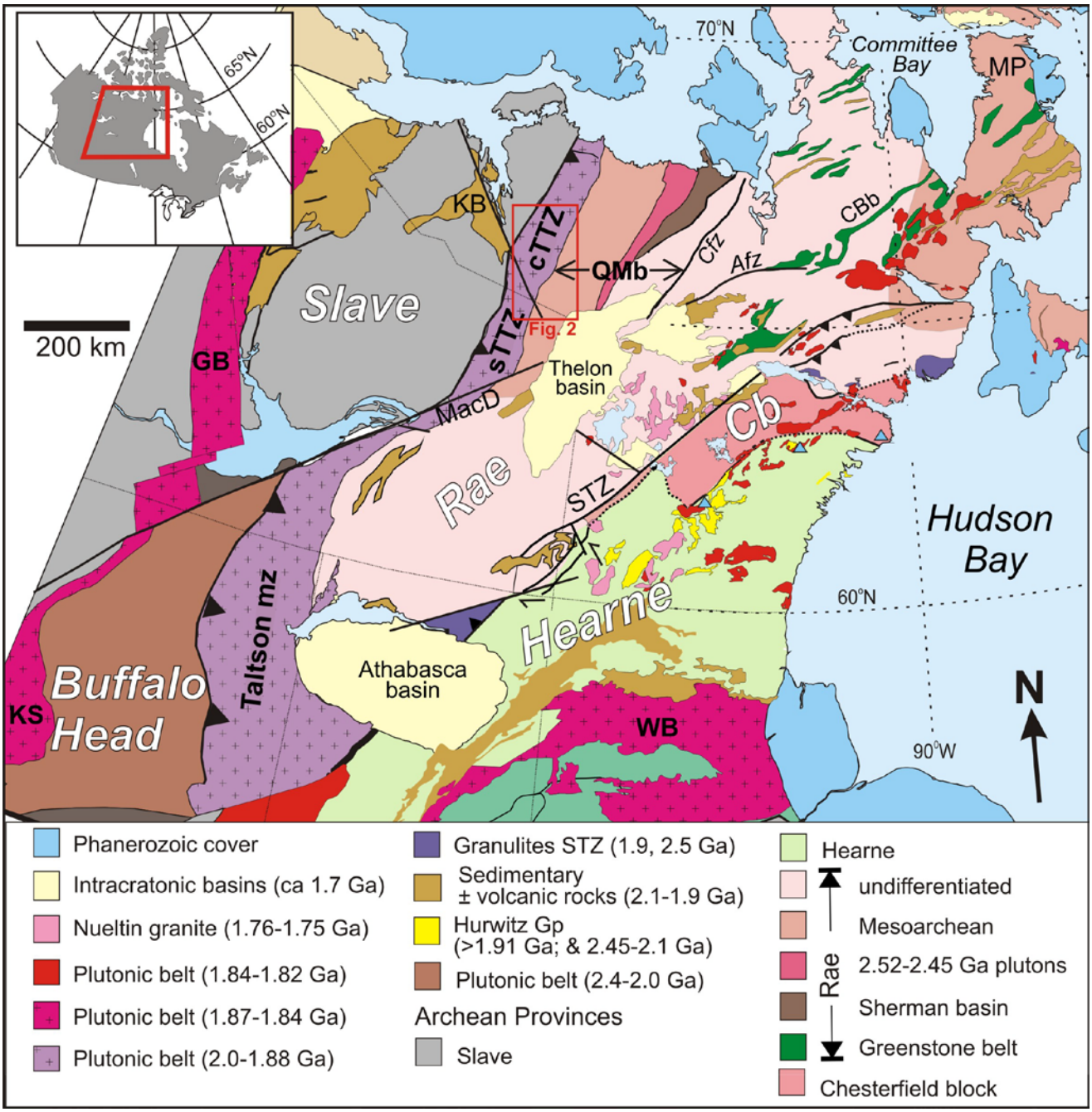

Figure 1. Regional geology adjacent to Thelon tectonic zone (modified from Berman *et al.*, 2005). Abbreviations: Afz = Amer fault zone, Cb = Chesterfield block, CBb = Committee Bay belt, Cfz = Chantrey fault zone, cTtz = central Thelon tectonic zone, GB = Great Bear, KB = Kilohigok basin, KS = Kitsuan, MacD = MacDonald fault, MP = Melville Peninsula, mz = magmatic zone, QMb = Queen Maud block, sTTZ = southern Thelon tectonic zone, STZ = Snowbird tectonic zone, WB = Wathanum Batholith. White box shows location of Figure 2. Red box in inset shows location of this figure in North America.

constraints in the context of recently acquired high-resolution aeromagnetic surveys (Natural Resources Canada, 2017) and isotopic data (Davis et al., 2013; 2014) which is ongoing. Ages reported below without reference are preliminary, unpublished results of W.J. Davis which are rounded to the nearest 10 Myr.

On west side of map sheet 76I (Fig. 2), the eastern Slave craton is dominated by metasedimentary and metavolcanic rocks of the Yellowknife Supergroup, and intruded by ca. 2.6 Ga granitoids (Frith, 1982; Thompson, 1986). Metamorphic grade increases eastward from lower- to upper-amphibolite facies, resulting from both Neoarchean and Paleoproterozoic (Thelon orogeny) events. This gradient culminates northeast of the Bathurst fault (Fig. 2), where migmatitic granitoid gneisses dominate and Yellowknife Supergroup (YSg) supracrustal rocks are absent (Thompson, 1986). Whereas Thompson (1986) considered these gneisses to reflect deeper crustal levels of Slave craton, Nd isotopic data (Berman et al., 2016, 2017), together with the absence of recognizable Yellowknife Supergroup metasedimentary rocks, suggest that they may represent a different crustal block. This region is referred to below as the Overby Lake domain (OLd; Fig. 2), whereas the region to the west is referred to as the YSg domain of the Slave craton.

The Overby Lake domain is bounded to the east by the westernmost of three Paleoproterozoic plutonic belts, but field relationships do not define whether the boundary is structural or intrusive due to high-strain and similar lithologies (quartz diorite, granodiorite, monzogranite) on both sides. Three belts of Paleoproterozoic, commonly orthopyroxene-bearing plutonic rocks, the western (Wpb), central (Cpb) and eastern (Epb) plutonic belts, are distinguished by three discrete linear high-amplitude aeromagnetic anomalies. They consist of a spectrum of compositions from gabbro to alkali feldspar granite, but early quartz diorite and late monzogranite or granodiorite is a common field relationship that is borne out by U-Pb zircon data (Berman et al., 2016, 2017; W.J. Davis, work in progress). Intense structural transposition makes it unclear whether primary contacts of magmatic belts are structural or intrusive.

Crystallization ages determined in the Wpb include 2010 Ma granodiorite, ca. 2000 Ma diorite, 1994 ± 4 Ma (Frith and van Breemen, 1990) K-feldspar megacrystic granodiorite that dominates the southern map sheet, and ca. 1990 Ma monzogranite. The occurrence of 2029 ± 5 Ma clinopyroxene-bearing quartz monzonite (L2; Davis et al., 2014) and 2020 Ma diorite (M157) indicates an older component in the Wpb. A ca. 2.02 Ga peak in the detrital zircon population of a < 1.95 Ga metapsammite in the adjacent Ellice River domain (Davis et al., 2018) suggests this older phase formed a significant component of the TTZ plutonism.

Figure 2 (opposite page). Simplified geological map of Thelon tectonic zone project area based on interpretation of aeromagnetic data (Natural Resources Canada, 2017) and previous work (Thompson et al., 1986; Frith, 1982) with 2014-2016 bedrock mapping (Berman et al., 2015, 2016) and geochronology (Davis et al., 2013, 2014, work in progress). Sample locations are shown with symbols explained in Figure 3. Legend also includes relevant sample symbols. Abbreviations: dm = domain, p.b. = plutonic belt, QMb = Queen Maud block, YSg = Yellowknife Supergroup.

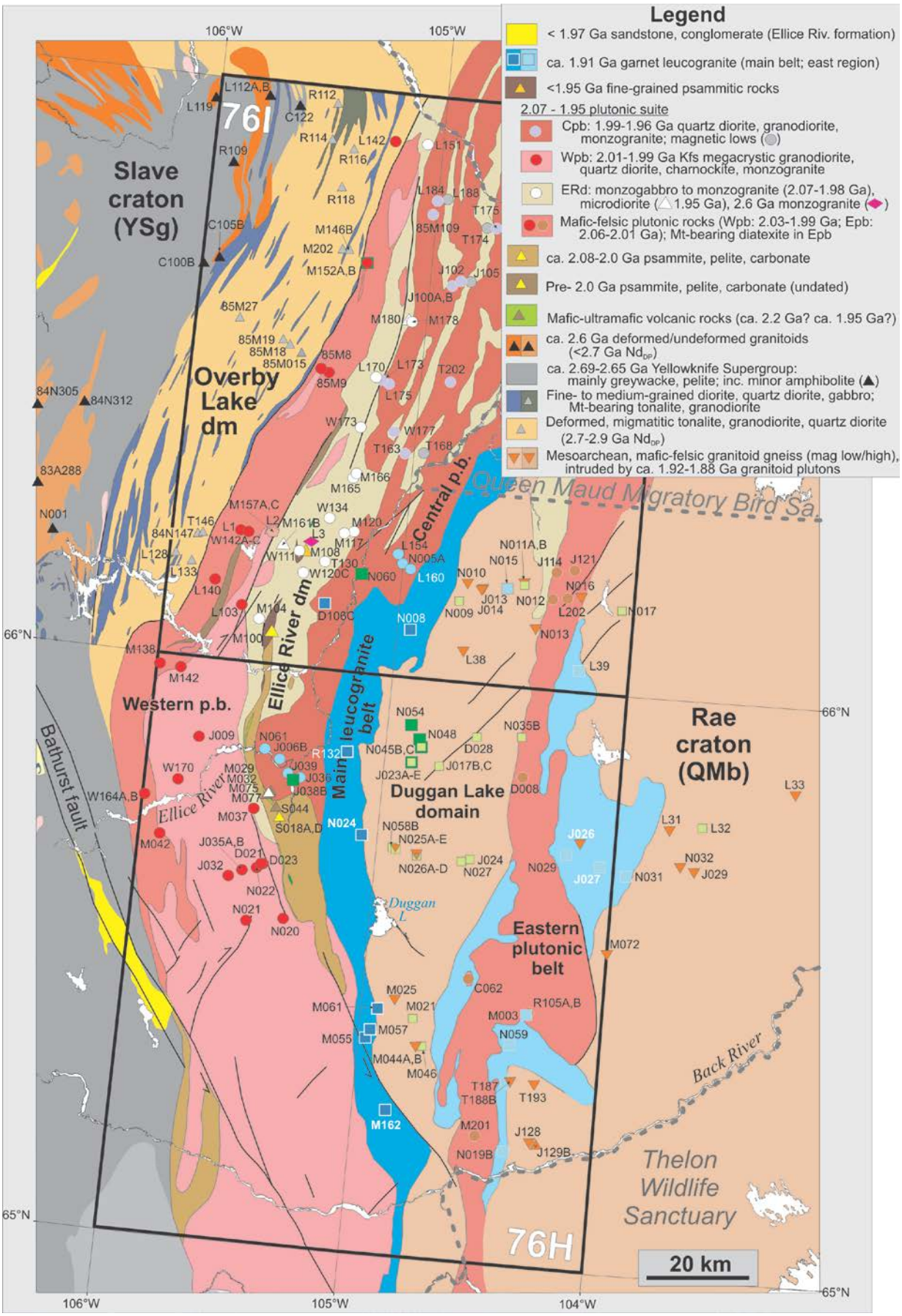
Legend
< 1.97 Ga sandstone, conglomerate (Ellice Riv. formation)
ca. 1.91 Ga garnet leucogranite (main belt; east region)
<1.95 Ga fine-grained psammitic rocks
2.07 - 1.95 plutonic suite
Cpb: 1.99-1.96 Ga quartz diorite, granodiorite, monzogranite; magnetic lows
Wpb: 2.01-1.99 Ga Kfs megacrystic granodiorite, quartz diorite, charnockite, monzogranite
ERd: monzogabbro to monzogranite (2.07-1.98 Ga), microdiorite (1.95 Ga), 2.6 Ga monzogranite
Mafic-felsic plutonic rocks (Wpb: 2.03-1.99 Ga; Epb: 2.06-2.01 Ga); Mt-bearing diatexite in Epb
ca. 2.08-2.0 Ga psammite, pelite, carbonate
Pre- 2.0 Ga psammite, pelite, carbonate (undated)
Mafic-ultramafic volcanic rocks (ca. 2.2 Ga? ca. 1.95 Ga?)
ca. 2.6 Ga deformed/undeformed granitoids (<2.7 Ga Nd$_{DP}$)
ca. 2.69-2.65 Ga Yellowknife Supergroup: mainly greywacke, pelite; inc. minor amphibolite
Fine- to medium-grained diorite, quartz diorite, gabbro; Mt-bearing tonalite, granodiorite
Deformed, migmatitic tonalite, granodiorite, quartz diorite (2.7-2.9 Ga Nd$_{DP}$)
Mesoarchean, mafic-felsic granitoid gneiss (mag low/high), intruded by ca. 1.92-1.88 Ga granitoid plutons
106°W
105°W
104°W
66°N
65°N
76I
76H
Slave craton (YSg)
Overby Lake dm
Ellice River dm
Central p.b.
Queen Maud Migratory Bird Sa.
Western p.b.
Bathurst fault
Ellice River
Main leucogranite belt
Duggan Lake domain
Duggan L.
Eastern plutonic belt
Rae craton (QMb)
Back River
Thelon Wildlife Sanctuary
20 km

There are fewer age constraints for the Cpb and Epb. In the Cpb, three samples of quartz monzodiorite, granodiorite, and tonalite have ages between 1980 and 1960 Ma, slightly younger than samples from the Wpb. Plutonism in the Epb is bracketed between 2070 Ma granodiorite in 76I and 2005 ± 5 Ma monzogranite in 76H (Davis et al., 2013). Whereas some gabbro and quartz diorite in the Epb is weakly deformed, other granitoid rocks are well foliated, and the belt is wider in the south, where it forms tight map-scale folds (Fig. 2). In several locations, the Epb is spatially associated with magnetite-bearing diatexite (Berman et al., 2015b; 2016) interpreted to be derived from iron-rich metasedimentary rocks.

East of the Epb, Mesoarchean (ca. 3.2 – 2.9 Ga) upper amphibolite to granulite-facies plutonic rocks of the Queen Maud block, western Rae craton, range in composition from quartz diorite to monzogranite (Schultz et al., 2007; Tersmette, 2012; Davis et al., 2013, 2014; Berman et al., 2015a). They typically display much shallower and more varied foliations than the TTZ, and consistently preserve evidence of reworking during the ca. 2.35 Ga Arrowsmith orogeny (Berman et al., 2005, 2013; Tersmette, 2012; Davis et al., 2014). Notably absent from this region are ca. 2.6 Ga plutonic rocks that are characteristically widespread across Rae craton further to the east (Hinchey et al., 2011 and references therein; Davis et al., 2014). West of the Epb, tonalitic rocks with ca. 3.4 – 3.1 Ga Nd model ages, 3.2 – 3.1 Ga U-Pb zircon crystallization ages, and ca. 2.35 Ga metamorphic zircon recrystallization, indicate that a previously poorly understood domain, informally referred to as the Duggan Lake domain, is part of the Queen Maud block. Lithologic and isotopic characterization of the Duggan Lake domain has two important outcomes: 1) the Epb is hosted by the Queen Maud block, western Rae craton; and 2) the >400 km-long magnetic low that coincides with the western margin of Duggan Lake domain reflects a major lithotectonic unit that defines the edge of Mesoarchean crust of the Queen Maud block (Berman et al., 2016, 2017). Geological mapping together with U-Pb zircon, Nd and oxygen whole rock isotopic data (Taylor et al., 2017) establish that the low-amplitude magnetic anomaly corresponds to variably strained, mostly garnet-bearing, peraluminous leucogranite that formed at ca. 1.93-1.91 Ga from melting of a sedimentary basin (Berman et al., 2015b, 2016, 2017).

Two other geochemically distinct, but aerially restricted plutonic suites are distinguished in the central TTZ. Low- to moderate-Zr, variably foliated monzogranite to alkali feldspar granite, dated at ca. 1.93 to 1.91 Ga intrudes the Duggan Lake domain and western Queen Maud block. High-Zr, ca. 1.90-1.89 Ga, post-tectonic quartz monzonite to monzogranite occurs as plutonic bodies in the Duggan Lake domain and as dykes, including a dyke cutting granulite-facies fabrics in the Cpb.

The affinity of crust in the Ellice River domain, a distinct magnetic low corresponding to a high proportion of supracrustal rocks between the Wpb and Cpb, is presently being further investigated. Formerly considered as potentially equivalent to the YSg (Frith, 1982), our new data support an emerging domain of Paleoproterozoic volcanic affinity. Dominated by metasedimentary rocks but including mafic to ultramafic volcanic rocks, the Ellice River

supracrustal belt, exposed in map sheet 76H and the southern part of 76I, is now established to consist of at least two Paleoproterozoic cycles (Davis et al., 2018). An older psammitic sequence deposited after 2.2 Ga and prior to 1.95 Ga, the age of a porphyritic sill (M32; Davis et al. 2018), is considered pre-Thelon in age, as it contains no ca. 2.0-1.98 Ga detrital zircons. This contrasts with a younger metasedimentary cycle with a maximum depositional age of 1.95 Ga, derived almost exclusively from unroofed Thelon-age rocks. Associated discontinuous, <1 km wide strands of ultramafic and mafic volcanic rocks (Berman et al., 2015b, 2016), some of which are spatially associated with polymetallic geochemical anomalies (e.g., Ag, Pb, Cu, Zn, Ni, U; McCurdy et al., 2013), are undated. The absence of exposed contacts between the different supracrustal rocks obscures relationships between the volcanic sequences and dated clastic rocks. However, preliminary Nd isotopic data (R. Berman, work in progress) suggest the volcanic rocks are Paleoproterozoic. .

North of recognizable supracrustal rocks in the Ellice River domain, quartz diorite to monzogranite plutonic rocks dominate the low-amplitude aeromagnetic anomaly, and preliminary geochronology results for two strongly foliated granodiorites are 2060 and 1980 Ma. The oxygen isotope signatures of Ellice River domain plutonic rocks suggest that their non-magnetic character is due to greater interaction with sedimentary rocks than plutonic rocks in the adjacent magnetic highs (Taylor et al., 2017). At one outcrop, gneissic monzogranite (sample L3 discussed in this report) has been dated at 2.6 Ga (Davis et al., 2014). As isotopic data for nearby rocks indicate that the aerial extent of Archean lithologies is very limited, we consider that this outcrop is part of a small structurally emplaced panel. For geochemical interpretation, it is important to note that sample L3 is considered a mixed lithology with pink monzogranite (ca. 1.9 Ga?) intrusive into Neoarchean quartz diorite.

Introduction to Thelon Tectonic Zone Geochemistry

All whole rock major and trace element analytical work included in this open file was carried out at Activation Laboratories Ltd., Ancaster, Ontario, Canada (http://www.actlabs.com/). Appendix 1 contains analyses of GSC internal standards and blind duplicates. Appendix 2 contains the quality control (QC) pages of Activation Laboratories for all the sample batches analyzed during this study. These pages contain information on analytical techniques, detection limits, results on calibration standards and duplicate samples runs. The location of TTZ geochemical samples collected during the 2012, 2014 and 2016 field seasons, as well as a subset of GSC archived samples, are shown in Figure 2. Sample information and analytical results are given in Appendix 3. Groupings of TTZ samples were made on the basis of field relationships, U-Pb zircon ages and geochemical characteristics, and are shown in Figure 3 along with corresponding symbols used in geochemical plots. Most of the sample groups are defined by spatial association (e.g., Wpb, Cpb, Epb; main leucogranite belt; Overby Lake domain), whereas high-Zr and normal-Zr, ca. 1.9 Ga plutonic rocks are geochemically defined. The majority of dated (U/Pb or Sm/Nd) Mesoarchean plutonic rocks are considerably less potassic than Paleoproterozoic rocks of the

same silica content (Figs. 4 and 5). Accordingly, some undated samples were assigned to geochemical groups on the basis of K_2O content.

Geochemical data for Archean rocks are shown in Figures 4a-8a and 9, whereas data for Paleoproterozoic rocks are shown in Figures 4b-8b (along with shaded fields encompassing the Archean rocks for comparison). As trace element variations can be closely correlated to silica content, Paleoproterozoic samples have been subdivided into those with greater than and less than 55 wt.% SiO_2 on primitive mantle normalized plots (Figs. 10 and 11).

Below, specific major and trace element features of each unit/group/suite/assemblage are described. Following this, the lithogeochemical character of basement and Paleoproterozoic plutonic rocks of the TMZ (Goff et al., 1986; Theriault, 1990; De et al., 2000) is assessed in comparison to the TTZ dataset.

Major and Trace Element Features of Thelon Tectonic Zone Igneous Units:

1. ***Archean plutonic rocks***.

Archean plutonic rocks collected from the study area are subdivided into four geographic domains/groups (see Figs. 2 and 3). From west to east, these are: (a) Slave craton - YSg domain , i.e., the western portion of Fig. 3 where YSg rocks are present; (b) Slave craton - Overby Lake domain (OL); (c) Ellice River domain (ER); and (d) Rae craton. Based on major element compositions (Fig. 4a and 5a), Archean samples can be split into lower and higher-K groupings with the former including Slave craton - Overby Lake domain (N=16) plus Rae medium-K samples (N=24), and the latter consisting of Slave craton-YSg domain samples (N=12), two Rae high-K samples and one 2.6 Ga Ellice River domain sample.

(a) Slave craton – Yellowknife Supergroup domain:

Archean plutonic rocks from the Slave-craton -Yellowknife SG domain (black triangles) are bimodal, consisting of gabbro-diorite to granodiorite and monzogranite to syenogranite (Fig. 4a), follow a calc-alkaline trend (Figs. 4a and 7a), and are medium-K to shoshonitic (Fig. 5a). The mafic samples are amphibolites, a volumetrically minor component, that could represent metamorphosed Proterozoic dyke rocks. Felsic (>55 wt.% SiO_2) samples are magnesian (Fig. 6a) and range to strongly peraluminous (aluminum saturation index (ASI)=1.15 to 1.25) (Fig. 8a), whereas mafic end-members are ferroan and metaluminous. Primitive mantle normalized trace element patterns for this group show a large range of abundances (Fig. 9a). More felsic (>55 wt% SiO_2) samples (N=8) exhibit positive Ba and pronounced negative Nb anomalies, along with variable Sr, P and Ti anomalies. Mafic samples (N=4) exhibit relatively unfractionated patterns compared to more felsic samples, with moderate negative Nb anomalies, and slight negative to no Sr, P and Ti anomalies.

(b) Slave craton - Overby Lake domain:

Overby Lake domain samples (light grey triangles) range from diorite to alkali-feldspar granite, but consist mainly of tonalite, and are calcic to calc-alkaline (Fig. 4a and 7a). This group is medium-K, magnesian and metaluminous to slightly peraluminous (Figs. 5a, 6a and 8a). Primitive mantle normalized patterns of more felsic (>55 wt.% SiO_2) samples are, in general, more depleted in LILE than either Slave Yellowknife or Rae basement samples of similar silica contents (Fig. 9b). They exhibit well-developed negative Nb anomalies, mainly positive Sr, Zr and Eu anomalies, with slight negative P and Ti anomalies, features which closely resemble those of high La/Yb suites, including Archean TTG suites. Patterns of more mafic samples (N=2) resemble those of more felsic samples but are less HREE-depleted.

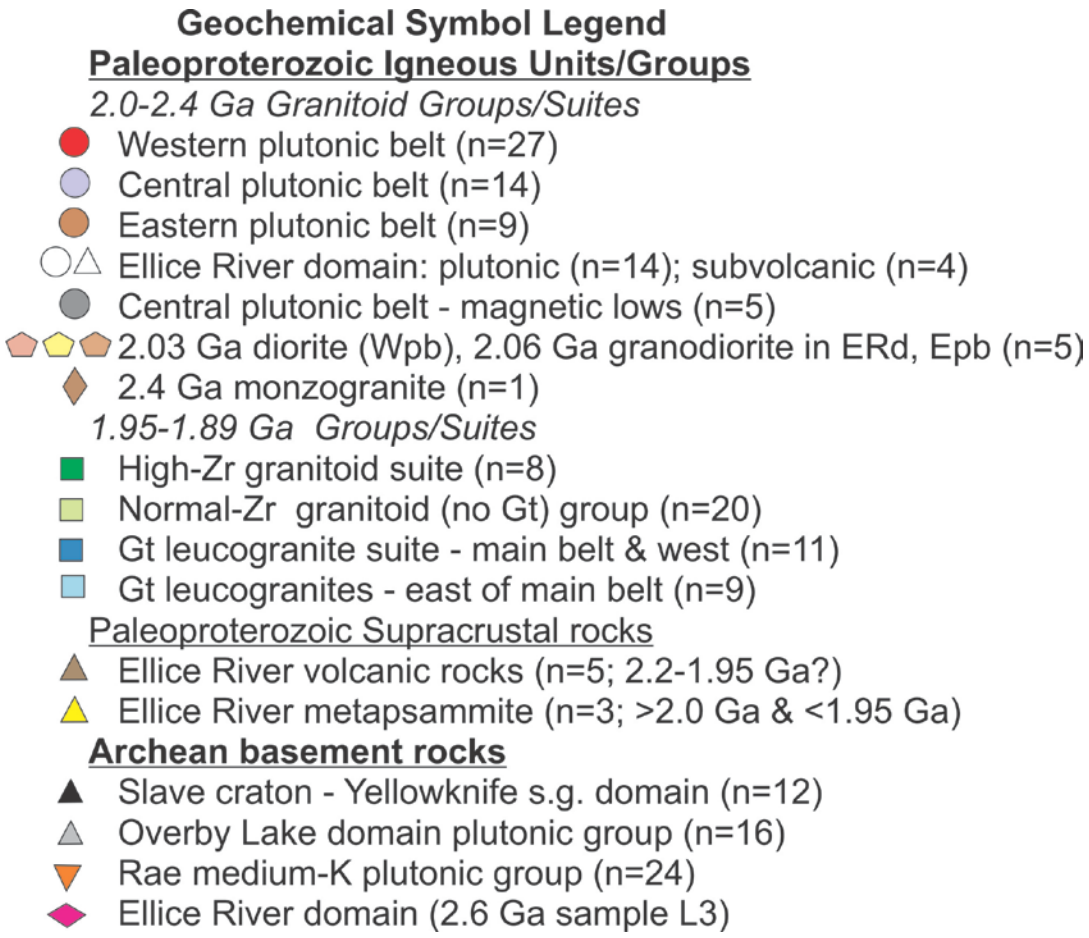

Figure 3: Igneous rock geochemical sample symbol legend

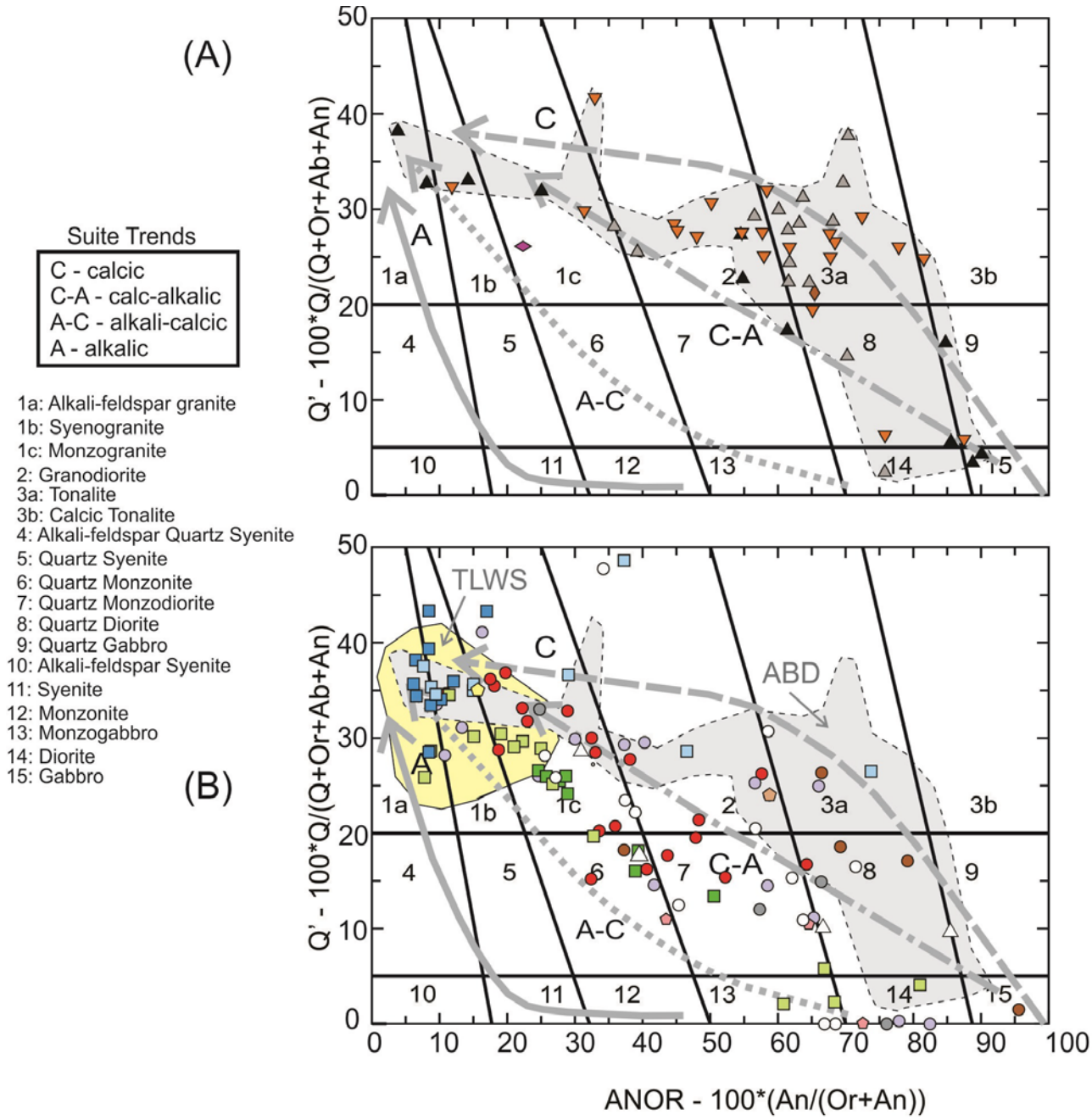

Figure 4. Thelon tectonic zone (TTZ): (a) Archean; and (b) Paleoproterozoic plutonic rock samples plotted on the normative Q' (100*(Q/(Q+Or+Ab+An)) versus ANOR (100*(An/(Or+An)) classification plot (Streckeisen and LeMaitre, 1979). Quartz-free to slightly undersaturated samples have been projected onto the X-axis. Samples are subdivided into various age and geochemical groups, as shown in the symbol legend (see Fig. 3) and discussed in the text. Also shown are fields for: combined four TTZ Archean basement domains (ABD, grey shaded field; see text) and most Taltson zone late western suite samples (TLWS, yellow shaded field). Compositional trends for different representative types of plutonic suites are from Whalen and Frost (2013).

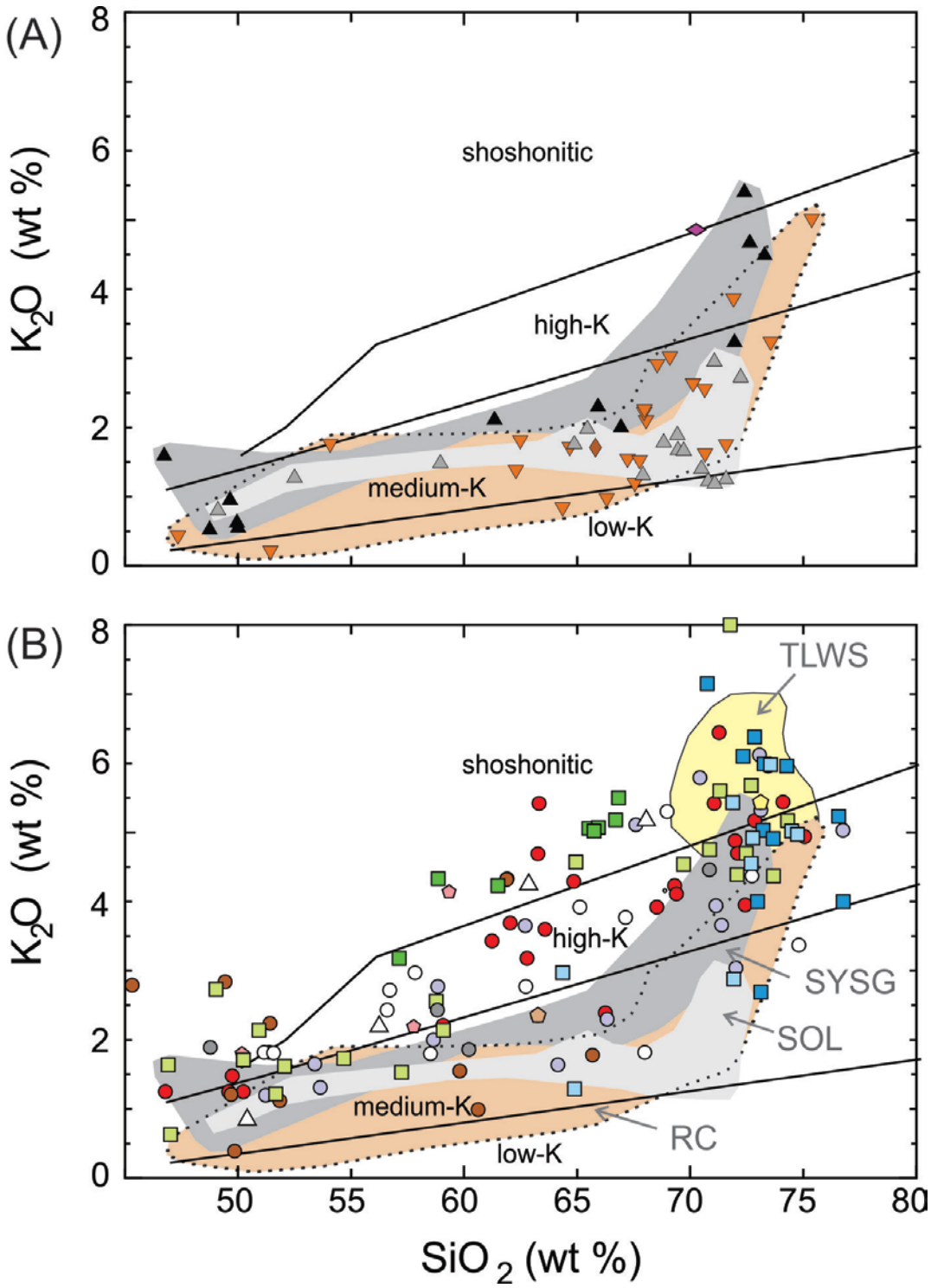

Figure 5. Thelon tectonic zone: (a) Archean; and (b) Paleoproterozoic plutonic rock samples plotted on a SiO_2 vs. K_2O plot with suite subdivisions after LeMaitre (1989) (low-, medium-, high-K) and Peccerillo and Taylor (1976) (high-K, shoshonitic). See Fig. 3 for symbol legend. Also shown are fields for: Archean basement domains (Slave – Yellowknife S.G (SYSG); Slave Oversby Lake (SOL); and Rae craton (RC) and the Taltson zone late western suite (TLWS).

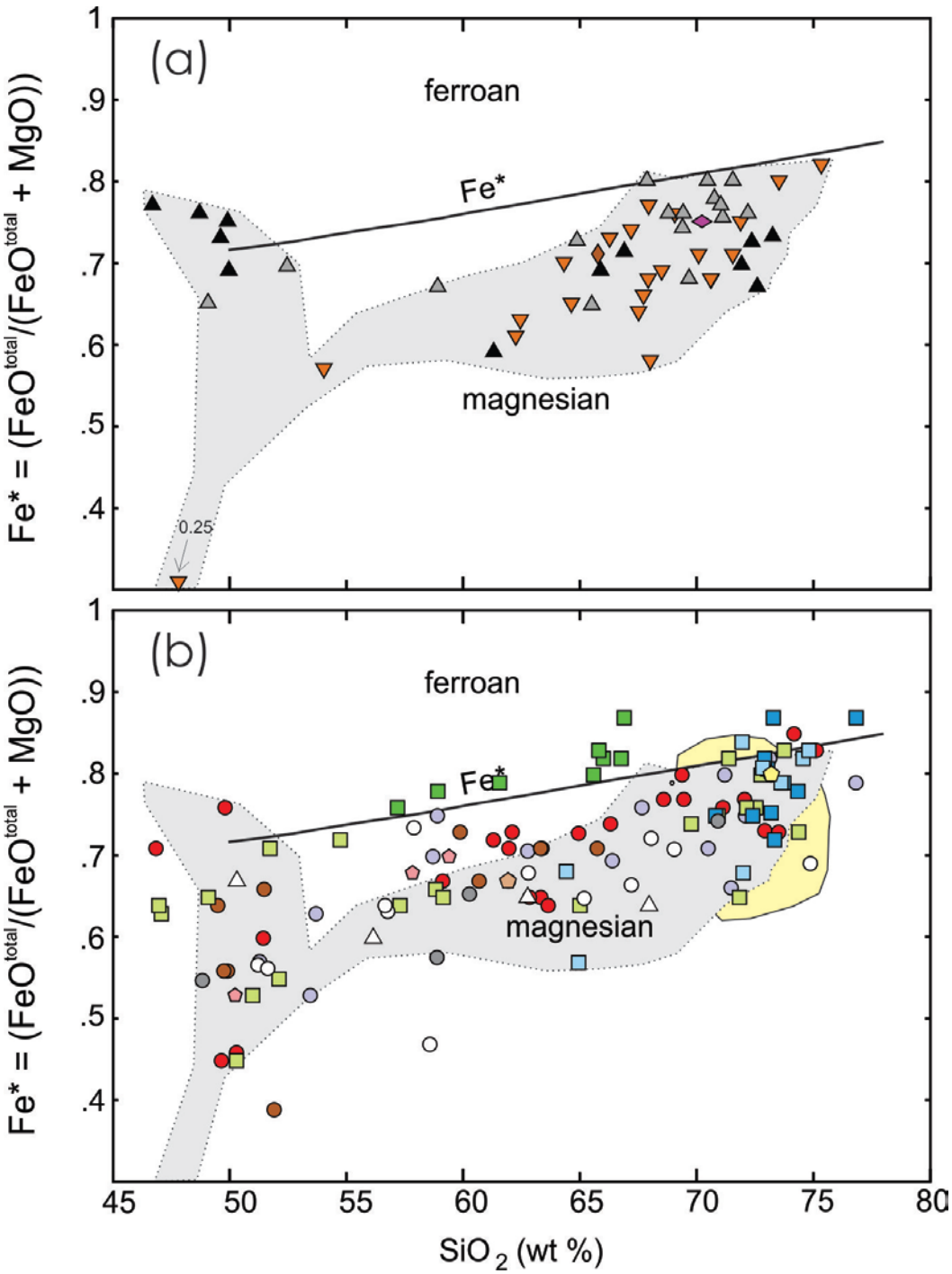

Figure 6. Thelon tectonic zone: (a) Archean; and (b) Paleoproterozoic plutonic rock samples plotted on the $FeO^{total}/(FeO^{total} + MgO)$ (or Fe*) vs. SiO_2 diagram of Frost et al. (2001, 2008). Symbols legend shown in Fig. 3 and shaded fields as in Fig. 4.

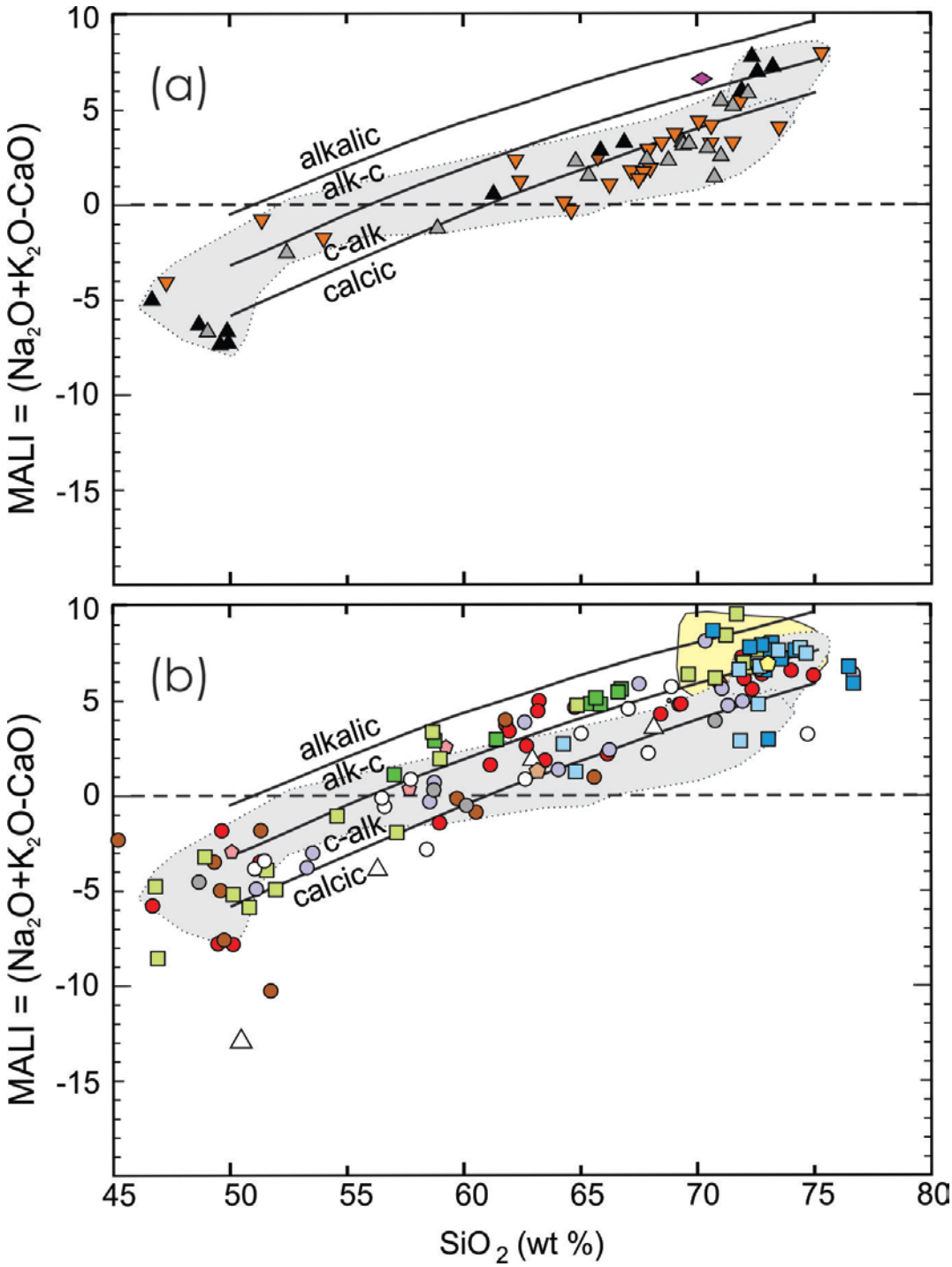

Figure 7. Thelon tectonic zone: (a) Archean; and (b) Paleoproterozoic plutonic rock samples plotted on the Na_2O+K_2O-CaO (or MALI) vs. SiO_2 granitic rock classification plots of Frost et al. (2001, 2008). Shown are ranges for alkalic-calcic, calc-alkalic, and calcic rock series. Symbols legend shown in Fig. 3 and shaded fields as in Fig. 4.

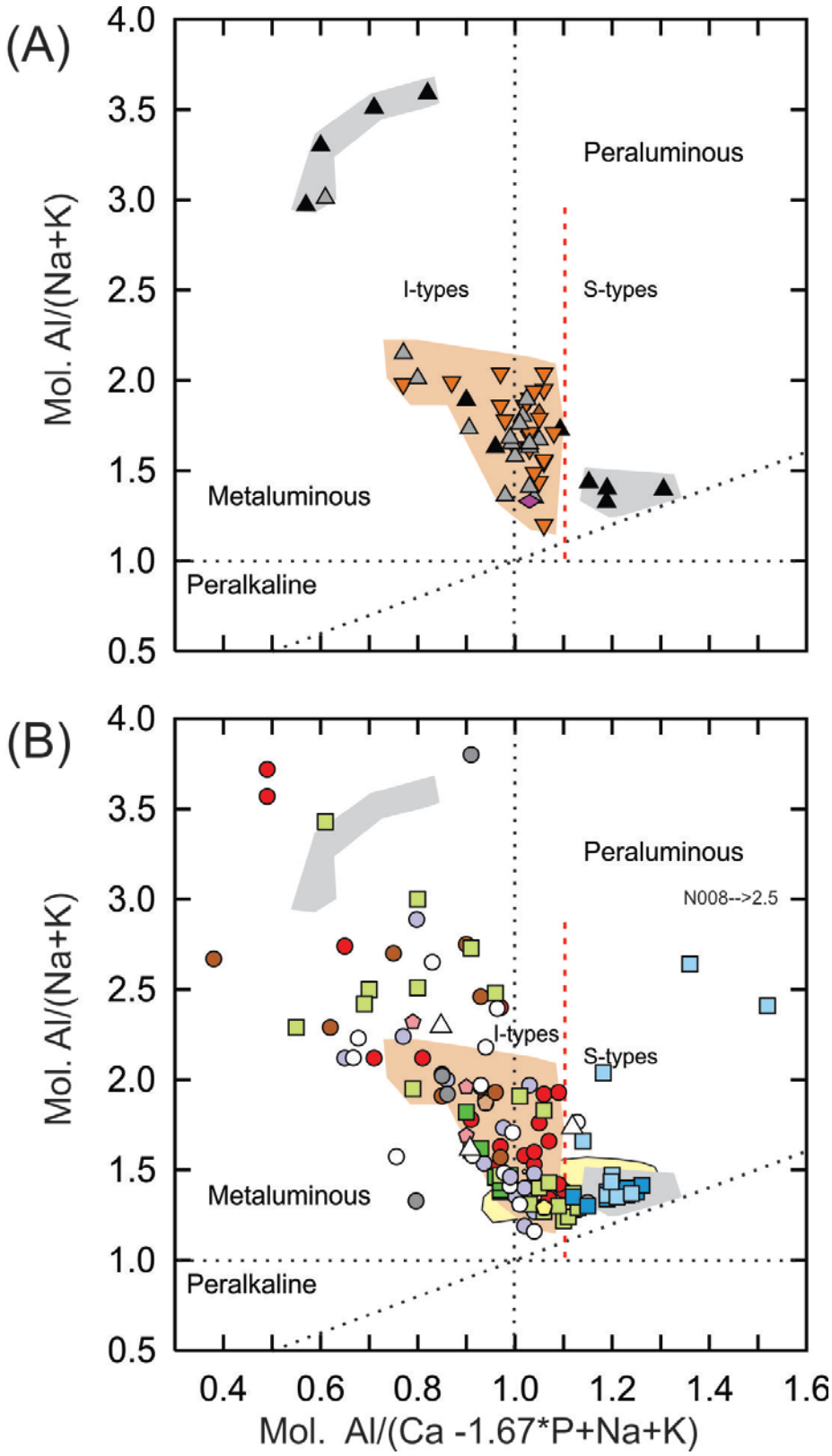

Figure 8. Thelon tectonic zone: a) Archean; and (b) Paleoproterozoic plutonic rock samples plotted on a Shand (1943) plot of Al saturation index (molecular Al/(Ca+Na+K-1.67*P)) versus alkali saturation index (molecular Al/(Na+K)) (modified after Maniar and Piccoli, 1989). Symbols legend shown in Fig. 3 and shaded fields as in Fig. 4. Also shown is the dividing line at ASI=1.1 between I- and S-type granites from White and Chappell (1983).

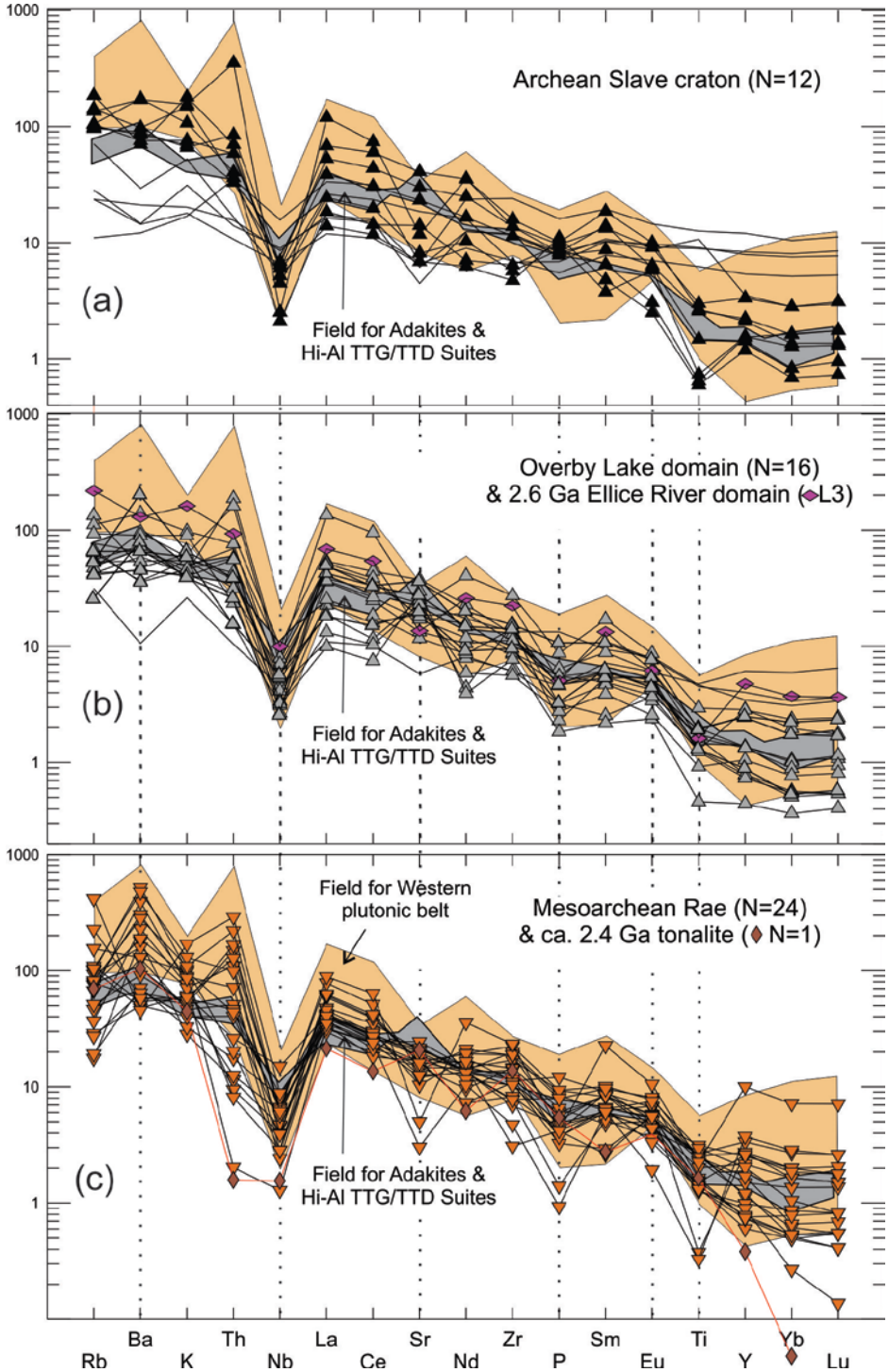

Figure 9. Thelon tectonic zone Archean igneous rock sample units/groups plotted on extended element primitive mantle normalized plots (spidergrams). Shown for comparison purposes are the fields for: (1) the felsic (>55% SiO_2) TTZ ca. 2.0 Ga Wpb subgroup derived from Fig. 10a (beige), and; (2) various high La/Yb suite averages (grey: Archean high-Al tronhjemite–tonalite–dacite (TTD), post-Archean adakite plus high-Al TTD and Cenozoic adakite), all from Drummond et al. (1996). Primitive mantle normalizing factors from Sun and McDonough (1989).

(c) *Rae craton domain (Queen Maud block):*

Rae craton plutonic samples (inverted orange triangles), representative of the western part of the Queen Maud block, range from diorite-gabbro to syenogranite, but consist mainly of granodiorite-tonalite (Fig. 4a). They follow a calcic to calc-alkaline trend (Figs. 4a and 7a), are magnesian and metaluminous to slightly peraluminous (Figs. 6a and 8a). Field relationships and U-Pb zircon dating of six samples suggest that felsic high-K phases post-date medium-K plutonic phases of this group. Normalized trace element patterns of more felsic (>55 wt.% SiO_2) samples (N=20) exhibit positive Ba and Th anomalies, well-developed negative Nb anomalies, variably developed negative Sr, P and Ti anomalies and a very large range in HREE abundances (Fig. 9c). Mafic (<55 wt.% SiO_2) Rae craton samples (N=4) have REE contents similar to the felsic samples but are more depleted in LILE's and LREE's. Overall this group's normalized patterns resemble Archean TTG suites, but the Rae samples are more enriched in LILE. Within the Rae craton domain, a late 2.4 Ga tonalite (N26C; brown diamond) plots between the calcic to alkali-calcic fields (Figs. 4a and 7a), is medium-K (Fig. 5a), magnesian (Fig. 6a) and slightly peraluminous (Fig. 8a). Its normalized trace element pattern (Fig**.** 9a) lacks Th enrichment relative to Nb, and shows depletion of HREE relative to LREE (i.e. high La/Yb).

(d) *Ellice River domain*:

One sample of Neoarchean (ca. 2.6 Ga) monzogranite in the Ellice River domain (L3; pink rhomb; interpreted as Neoarchean mafic plutonic rock intruded by ca. 1.9 Ga granitoid) plots at the felsic end of the alkali-calcic trend (Figs. 4a and 7a), is high-K to shoshonitic (Fig. 5a), magnesian (Fig. 6a) and slightly peraluminous (Fig. 8a). The sample's normalized trace element pattern closely resembles, but is slightly more enriched than Overby Lake samples (Fig. 9b). In this regard its normalized pattern is more akin to Slave - YSg samples (Fig. 9a).

2. *ca. 2.0 Ga TTZ granitoid groups and units*

(a) The *Wpb group (red circles, n=27)* consists predominantly of K-feldspar porphyritic hb-bt monzogranite to granodiorite, but also includes quartz monzonite, quartz monzodiorite and diorite (red circles; Fig. 4b). The group plots between calc-alkaline and alkali-calcic trends (Figs. 4b and 7b) and is high-K to shoshonitic (Fig. 5b). Except for two mafic samples, this group is magnesian (Fig. 6b) and metaluminous to slightly peraluminous (Fig. 8b).

Higher silica (>55 wt.%) Wpb samples can be distinguished by Th contents, with the high Th group having mainly higher Rb and LREE, but with overlapping abundance ranges in P through Lu (Fig. 10a). Otherwise, normalized patterns for more felsic Wpb subgroup are similar, all exhibiting negative Nb, P and Ti anomalies and variable Sr anomalies. The compositional ranges of this subgroup are shown as beige shaded fields on all the normalized plots, including those of Archean samples (Fig. 9), as a visual aid to comparing variations in abundances between sample groups/units. The four mafic (<55 wt.% SiO_2) samples from the Wpb subgroup exhibit very similar normalized patterns to the low-Th felsic samples (Fig. 10a), with LILE and LREE

contents at the lower end of the range, moderately well-developed negative Nb anomalies, and irregular Sr, P and Ti anomalies (Fig. 11a).

(b) *Cpb samples corresponding with magnetic highs (light blue circles; n=14)* consist of magnetite-bearing syenogranite-alkali feldspar granite, granodiorite and quartz monzodiorite-diorite (Fig 4b). This group spans medium-K to shoshonitic fields (Fig. 5b) and calcic to alkali-calcic trends (Figs. 4b and 8b), and is magnesian (Fig. 6b) and metaluminous to peraluminous (ASI>1.1; Fig. 8b). Primitive mantle normalized patterns for the ten higher silica (>55 wt.%) samples exhibit similar features to the Wpb both in high- and low-Th subgroups (Fig. 10b). The three mafic (<55 wt.% SiO_2) intrusive rocks from the Cpb are more depleted than felsic members, with slight LILE enrichment, poorly developed Nb anomalies (Th~Nb) and variable P and Ti anomalies (Fig. 11b).

(c) *Cpb samples corresponding with magnetic lows (grey circles; n=5)* comprise diorite to monzogranite (Fig. 4b), are magnesian (Fig 6b), mainly calc-alkalic (Fig. 7b), medium- to high-K (Fig. 5b) and metaluminous (Fig. 8b). These samples exhibit poorly developed Nb (Th~Nb), Sr, P and Ti anomalies and a significant range in HREE abundances (Fig. 10b). The normalized patterns of individual rocks are comparable to the main group of Cpb rocks (Fig. 10b).

(d) The *Epb group (brown circles; n=9)* consists of quartz monzonite, tonalite, diorite to gabbro (Fig. 4b), ranges from calcic to alkali-calcic (Figs. 4b and 7b) and from medium-K to shoshonitic (Fig. 5b). It is magnesian and metaluminous (Figs. 6b and 8). Normalized patterns of the four higher silica (>55 wt.%) samples differ from the Wpb in being variably depleted in LILE and less enriched in Th relative to Nb (Fig. 10b, c), with one sample with Th<Nb, (i.e. poor developed negative Nb anomalies). Otherwise, their patterns are gently sloping, HREE depleted, without significant anomalies. The five mafic (<55 wt.% SiO_2) plutonic sample patterns are quite similar to felsic samples of this group, with poorly developed negative Nb and variable P and Ti anomalies (Fig. 11b).

(e) *Ellice River domain plutonic samples (open circles; n=14)* consist of quartz diorite-monzogabbro, granodiorite and monzogranite that define a calc-alkaline trend on the Q-ANOR plot (Fig. 4b), but cross the calcic to alkali-calcic fields on the MALI plot (Fig. 7b). The samples span the low-K to shoshonitic fields (Fig. 5b), are magnesian (Fig. 6b) and mostly metalumious to slightly peraluminous (ASI<1.1; Fig. 8b). Normalized trace element patterns of this group coincide with those of the Wpb, but display variable Sr, P and Ti anomalies (Fig. 10d).

(f) *2.07 – 2.02 Ga samples (n=5)* from the Wpb, ERd and Epb display geochemical characteristics that overlap closely with ca. 2.0 Ga plutonic rocks from these same domains on the various major element plots (Figs. 4b to 8b) and in their normalized patterns (Fig. 10a,b,d, 11a). The only exception is the low Th of M165 (Epb), which may relate to its mobility during hydrothermal alteration which is indicated by its oxygen isotopic composition (Taylor et al., 2017) and strong epidote overprint.

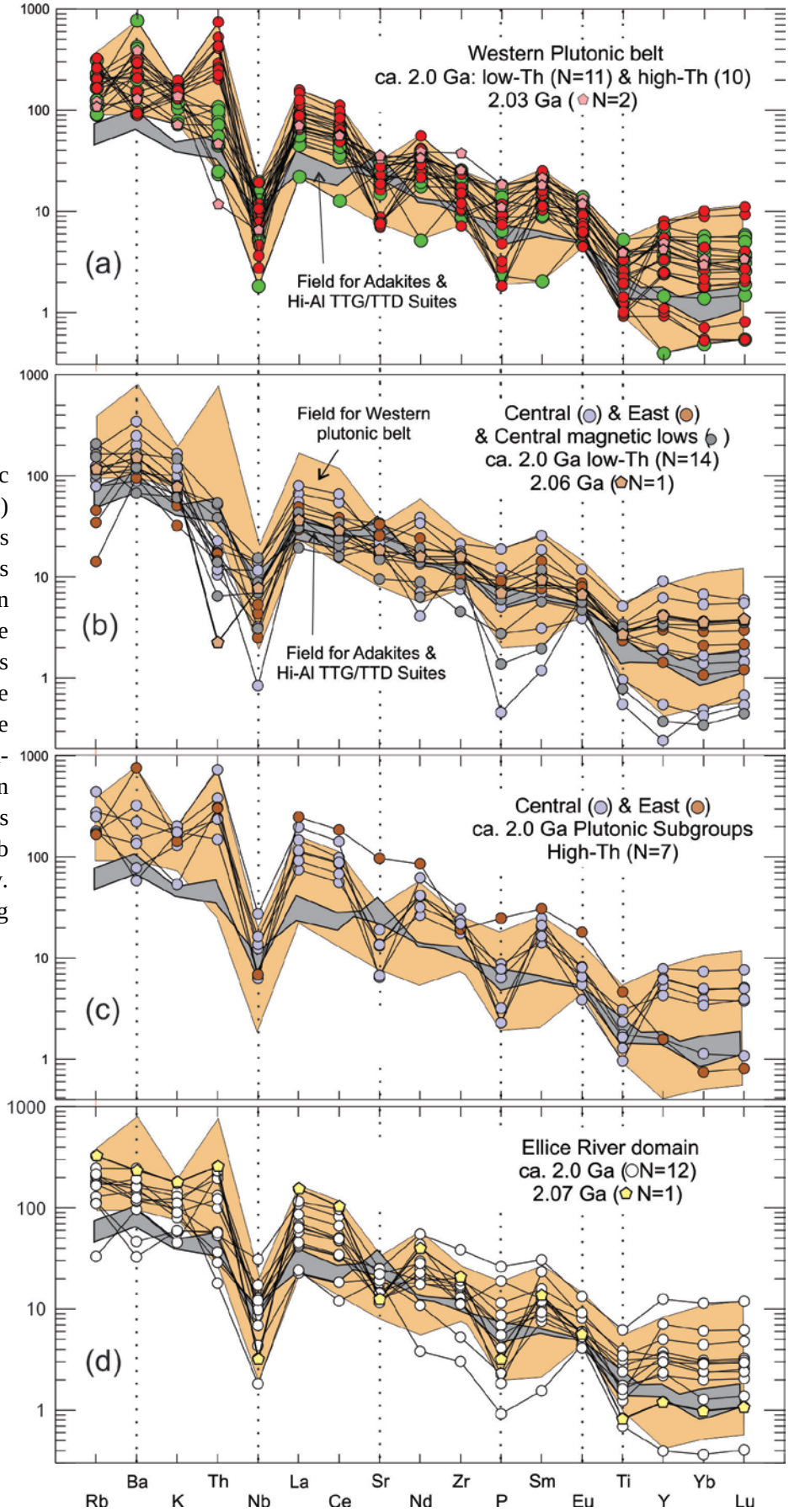

Figure 10. Thelon tectonic zone felsic (>55 wt.% SiO_2) Paleoproterozoic igneous rock sample units/groups (see Fig. 3) plotted on extended element primitive mantle normalized plots (spidergrams). To facilitate discussion, samples have been subdivided into high- and low-Th groupings; in 10a green and red circles are low and high-Th Wpb samples, respectively. Fields and normalizing factors as in Fig. 9.

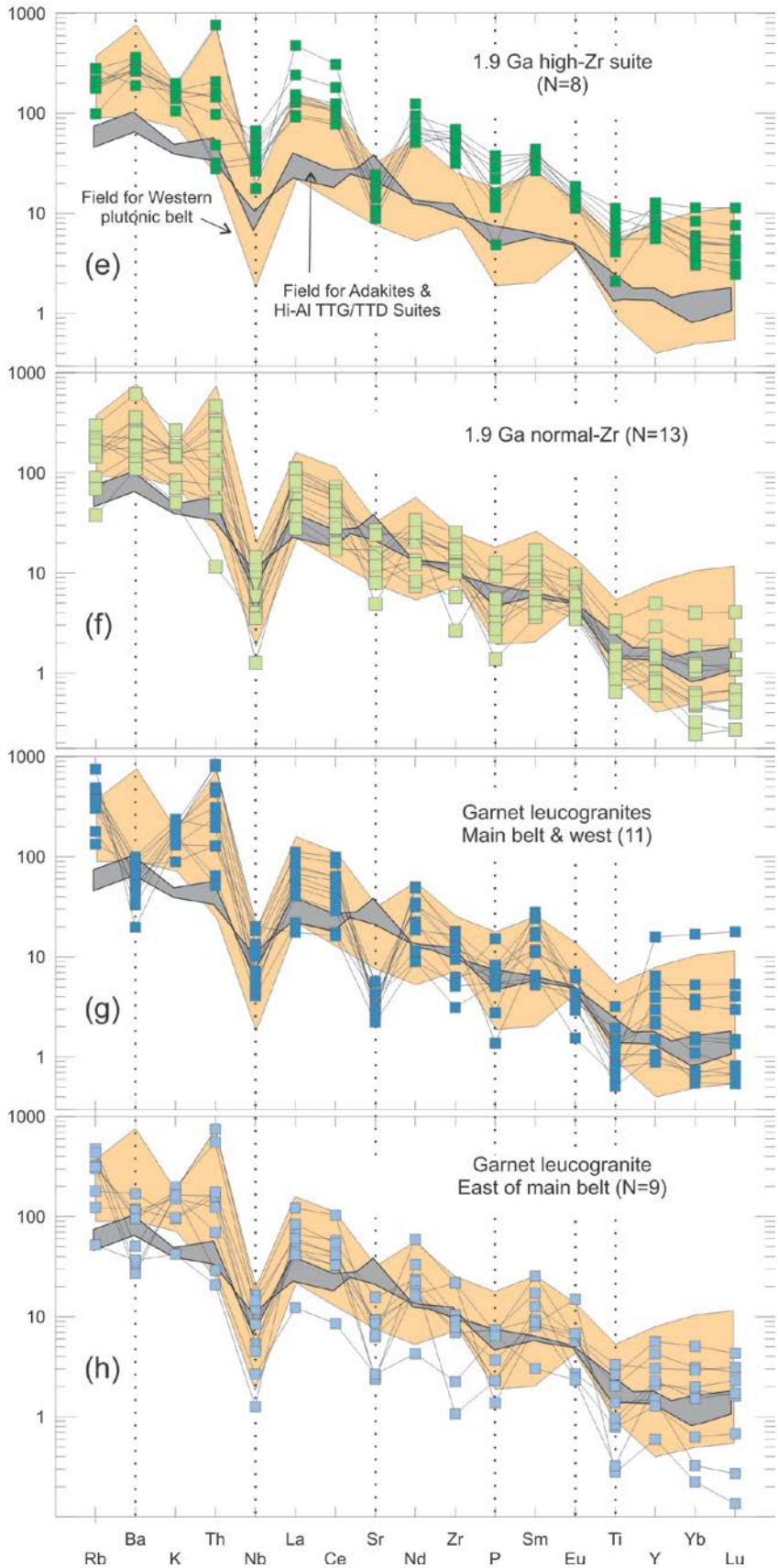

Figure 10. Thelon tectonic zone felsic (>55 wt.% SiO_2) Paleoproterozoic igneous rock sample units/groups (see Fig. 3) plotted on extended element primitive mantle normalized plots (spidergrams). To facilitate discussion, samples have been subdivided into high- and low-Th groupings; in 10a green and red circles are low and high-Th Wpb samples, respectively. Fields and normalizing factors as in Fig. 9.

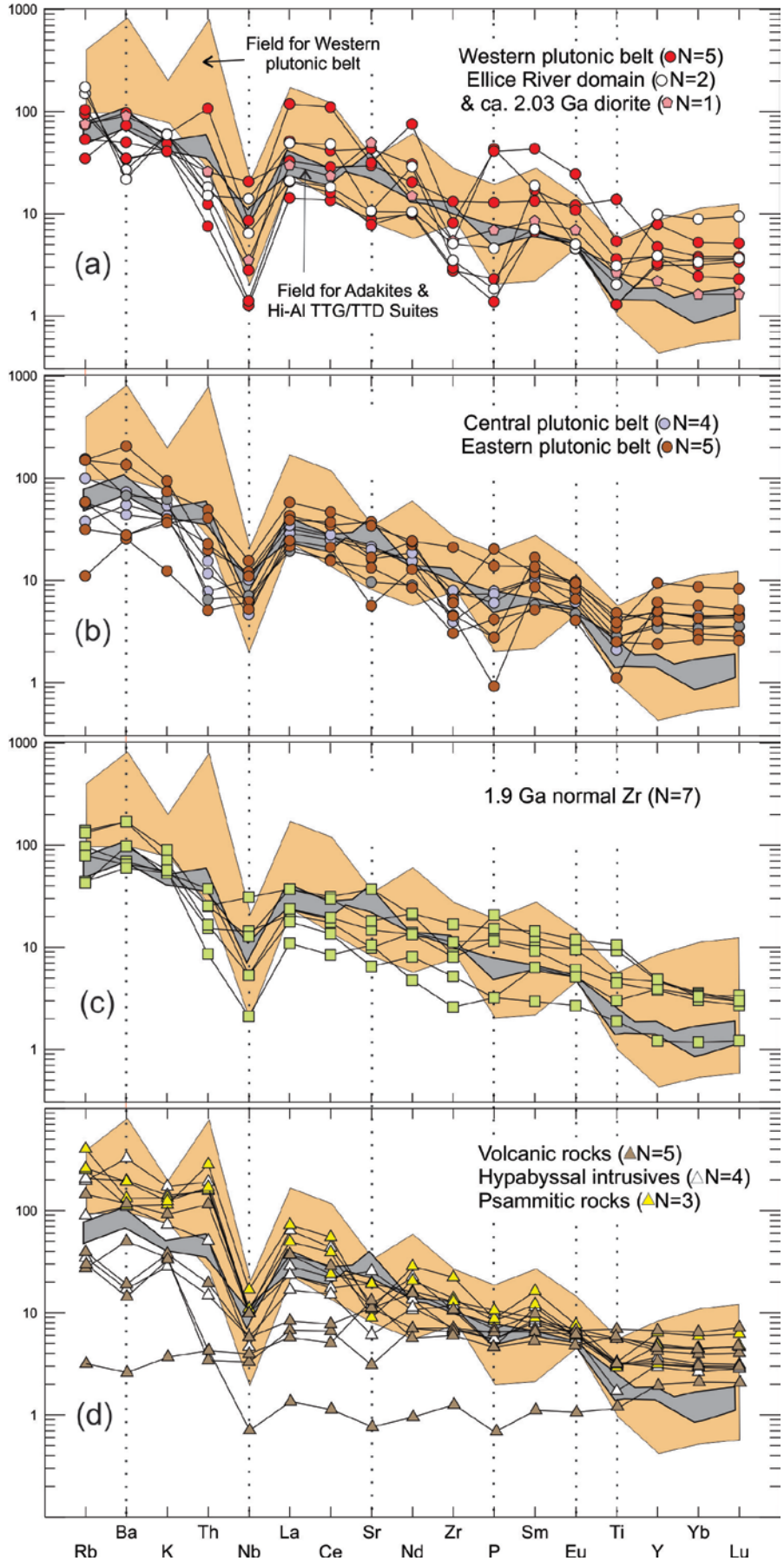

Figure 11. Thelon tectonic zone Paleoproterozoic rock sample units/groups (see Fig. 3) for mafic (<55 wt.% SiO_2) rocks (a-c) and supracrustal rocks (d) plotted on extended element primitive mantle normalized plots (spidergrams). Subdivisions, fields and normalizing factors as in Fig. 10.

3. *1.93-1.89 Ga TTZ suites*

(a) The *high-Zr granitoid samples* (dark green squares; n=8) span a compositional range from quartz monzodiorite to monzogranite and define a trend intermediate between alkali-calcic and calc-alkali (Figs. 4b and 7b). This suite is characterized by quite linear intermediate composition (SiO_2= 57-67 wt.%) shoshonitic trend (Fig. 5b), plots exclusively in the ferroan field (Fig. 6b) and is metaluminous (ASI<1.0; Fig. 8b). Except for Th, normalized trace element contents of this suite are remarkably similar, with well-pronounced negative Sr and slight to pronounced negative P and Ti anomalies, and variable Nb/Th (Fig. 10e). Relative to the Wpb, this suite exhibits flatter patterns and is significantly enriched in REE and Zr.

(b) The *normal-Zr granitoid group samples* (light green squares; n=20*)* include dykes and sills of diorite to alkali-feldspar granite composition (Fig. 4b) that primarily cut the Mesoarchean Duggan Lake domain. These samples exhibit the same alkali-calcic to calc-alkali trend as the high-Zr suite (Figs. 4b, 7b), with highly variable K contents ranging from medium-K to strongly shoshonitic (Fig. 5b). All samples plot in the magnesian field (Fig. 6b) and are metaluminous to slightly peraluminous (ASI<1.1) (Fig. 8b). Normalized trace element patterns of 13 felsic (>55 wt.% SiO_2) samples (Fig. 10f) are similar to those of the Wpb, with pronounced negative Nb, Sr, P and Ti anomalies. Six mafic samples are relatively depleted in LILE and display only variable Nb (Fig. 11c). Mafic components of this group remain undated and could be pre-1.9 Ga in age.

(c) G*arnet leucogranites within and west of the main leucogranite belt* (medium blue unit, Figure 2; medium blue squares, n=11) consist of monzogranite to syenogranite, plot at the evolved end of non-alkalic trends on the Q-ANOR plot (Fig. 4b) and transect the calcic to alkalic fields on the MALI plot (Fig. 7a). This group is felsic (>70% SiO_2), medium-K to shoshonitic (Fig. 5b), mainly magnesian to slightly ferroan (Fig. 6b) and strongly peraluminous (ASI~1.2, Fig. 8b). These rocks exhibit similar primitive mantle normalized trace element patterns with very pronounced negative Ba, Nb and Sr anomalies and less pronounced negative P and Ti anomalies (Fig. 10g).

(d) *Garnet leucogranites* e*ast of* the *main belt* (light blue squares, n=9) are tonalitic to syenogranitic (Fig. 4b), magnesian (Fig. 6b), calcic to alkali-calcic (Fig. 7b) and span the medium-K to shoshonitic fields (Fig. 5). Samples are moderately (~1.1) to strongly (>1.3) peraluminous (Fig. 8b). Their normalized trace element patterns closely resemble those of the main leucogranite suite, with similar variability in LILE's, Th, Nb and REE's (Fig. 10h).

4. Ellice River domain supracrustal rocks and hypabyssal intrusives

*Ellice River volcanic rock*s include basaltic and peridotitic komatites (brown triangles; Fig. 12, n=5). Four samples exhibit consistent flat patterns with slight LILE and LREE enrichment and no, or poorly developed, negative Nb and Sr anomalies (Fig. 11d). In contrast, one sample (S044A) has a depleted pattern with negative Nb, Sr and P anomalies (Fig. 11d) that is similar to that of Ellice River domain plutonic rocks (Fig. 11a) and hypabyssal intrusives (Fig. 11d).

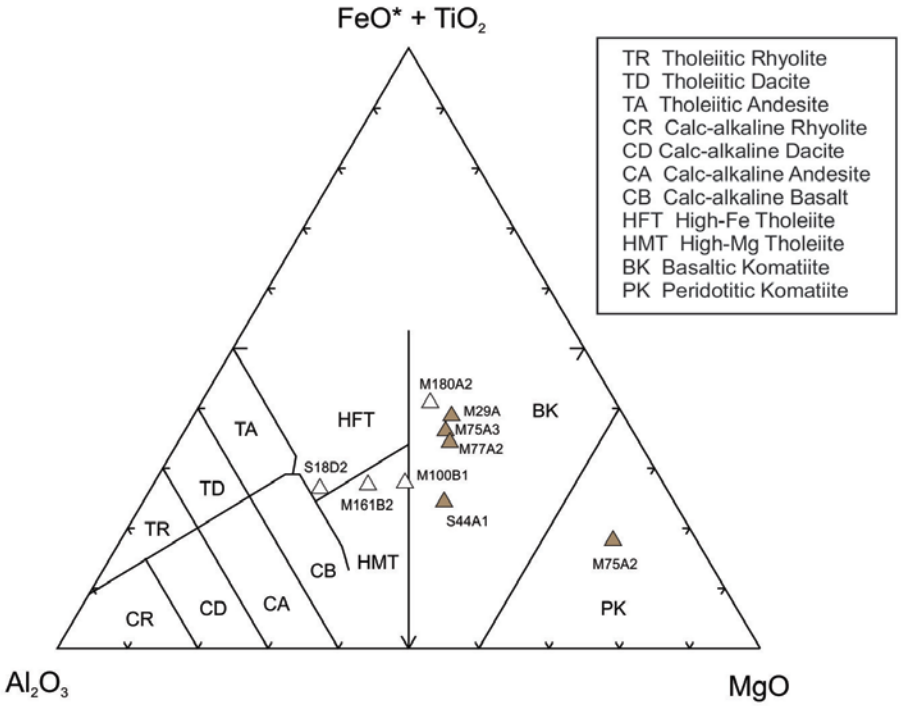

Figure 12. Thelon tectonic zone Paleoproterozoic volcanic and hypabyssal rock samples plotted on the cation volcanic rock classification plot of Jenson (1976).

<u>Tectonomagmatic Characterization of TTZ Paleoproterozoic Igneous Units</u>

The objective in this section is to characterize the Paleoproterozoic evolution of the central TTZ based on the tectonomagmatic signatures of its preserved Paleoproterozoic igneous rocks. Within a continent-continent collisional zone, pre-collisional oceanic and rift (MORB or OIB-like), subduction-related (arc-like) and post-collisional igneous rocks, such as those generated by slab-failure (SF-like) or delamination, could be preserved (c.f. Hildebrand and Whalen, 2015). All igneous rock samples (i.e., those with > and <55 wt.% SiO_2) are plotted on Figures 13 to 15, whereas only those with <55% SiO_2 are plotted on a number of basaltic rock tectonomagmatic trace element diagrams (Figure 16). For the purpose of comparison, Rae basement igneous rocks are shown as fields. Their petrogenesis is not considered in this section.

1. ca *2.06-1.96 Ga TTZ granitoid groups*

(a) *Wpb samples* plot in the volcanic arc granite (VAG) field in the Rb vs Y+Nb plot (Fig. 13a), and in the area of overlap between VAG and post-COLG (collisional granite) fields. On the Nb vs Y and Ta vs Yb plots (Figs. 13 b,c) and slab failure (SF) ratio plots (Figs. 14 and 15), about half exhibit low SF ratio values in the arc field and half have higher ratios in the SF field. Four <55% SiO_2 samples from the Wpb plot in normal arc fields in Fig. 16 and one sample shows an E-MORB or continental tholeiite affinity.

(b) *Cpb magnetic-bearing samples* plot between the VAG and post-COLG fields on the Rb vs Y+Nb plot (Fig. 13a). About 50% plot in slab failure fields, with the remainder plotting in the arc field, lacking high SF ratio values (Figs. 13b, c, 14, 15). Two <55% SiO_2 samples from the Cpb plot in normal arc fields, while one mafic sample has an E-MORB (non-arc) affinity.

(c) *Cpb non-magnetic samples* plot mainly in the post-COLG field on the Rb vs Y+Nb plot (Fig. 13a). All samples straddle the SF and arc fields on Nb vs Y and Ta vs Yb plots (Fig. 13b,c) and vary from SF-like to non-SF like in trace element ratio values (Fig. 14, 15).

(d) *Epb group samples* plot in the VAG field on the Rb vs Y+Nb plot and the SF and arc fields on the Nb vs Y and Ta vs Yb plots (Fig. 13). Consistent with their behaviour on normalized plots (Fig. 10b), five samples of this Epb subgroup display SF signatures for most ratios whereas the other five samples are characterized by lower arc-like ratios (Figs. 14, 15). In Figure 16, five samples display normal arc signatures, while one mafic sample displays E-MORB (non-arc) affinity.

(e) *Ellice River domain plutonic rocks* plot between the VAG and post-COLG fields, except one sample that plots in the syn-COLG field (Fig. 13a). On Nb vs Y, and Ta vs Yb plots (Figs. 13b, c), the three felsic samples plot in the SF field, whereas the nine quartz diorite-monzogabbroic samples plot both in the SF and arc fields. On trace element SF ratio plots, this group spans a large range of values, with about 50% displaying SF-type signatures for all ratios whereas the rest (L170A, M117A, M120A, M166A, W110A, W120B, W134A, W173A) exhibit notably lower Sr/Y ratios of <20 (Figs. 14 and 15). One of two mafic samples belonging to this group exhibit normal arc trace element signatures (sample M178), whereas another (sample W120C) is alkalic (non arc-like) (open circles, Fig. 16).

(f) *2.07 – 2.02 Ga samples* from the Wpb and Epb plot in the VAG and narrowly into the post-COLG fields on the Rb vs Y+Nb plot (Fig. 13a), whereas the ERd sample (M165) has higher Rb and plots in the syn-COLG field. All samples plot in the arc fields on Nb vs Y and Ta vs Yb plots (Fig. 13,b,c), except for M165 on the latter diagram. All samples display high SF-like values for all but Nb/Y (Figs. 14 and 15).

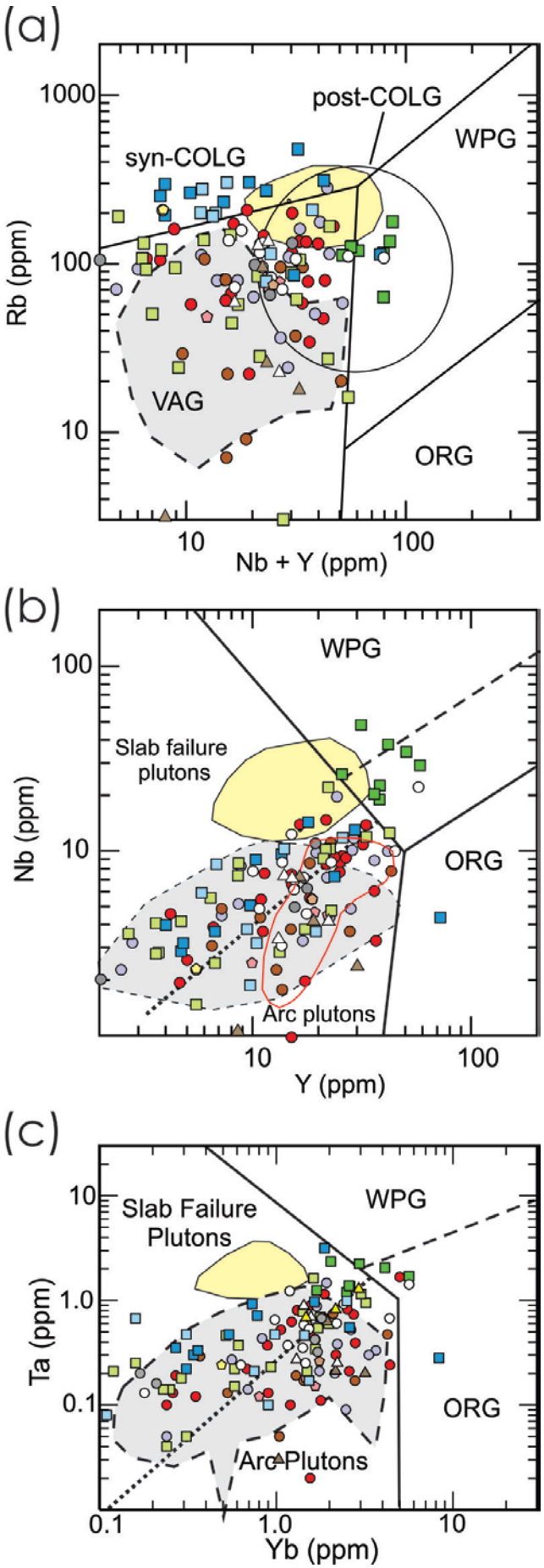

Figure 13. Paleoproterozoic Thelon tectonic zone igneous rock samples plotted on: (a) Rb vs Y+Nb; (b) Nb vs Y; and (c) Ta vs Yb granitoid tectonomagmatic discrimination plots; (a) from Pearce (1996); (b) and (c) from Pearce et al. (1984), modified by Hildebrand and Whalen (2015) by addition of arc and slab failure fields. Abbreviations: syn-COLG (syn-collisional granites); post-COLG (post-collisional granites); VAG (volcanic arc granites); WPG (within-plate granites); and ORG (ocean-ridge granites). Symbols legend shown in Fig. 3; shaded fields as in Fig. 4; red curve outlines Ttz mafic rocks with 55 - 60 wt. % SiO2.

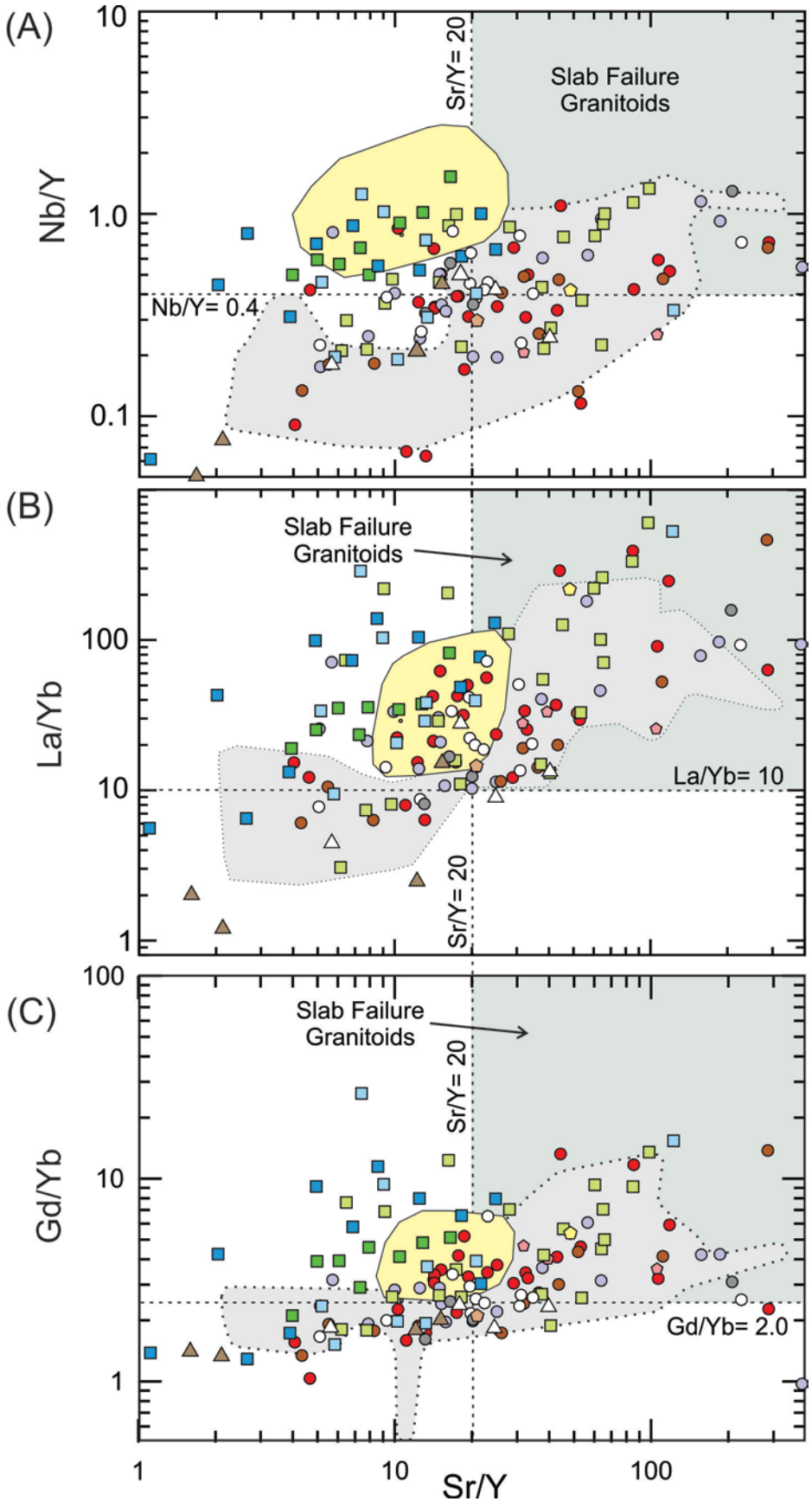

Figure 14. Paleoproterozoic Thelon tectonic zone igneous rock samples plotted on Sr/Y vs (a) Nb/Y, (b) La/Yb, and (c) Gd/Yb slab-failure (SF) vs arc magmatism discrimination plots of Hildebrand and Whalen (2015). Symbols legend shown in Fig. 3 and shaded fields as in Fig. 4.

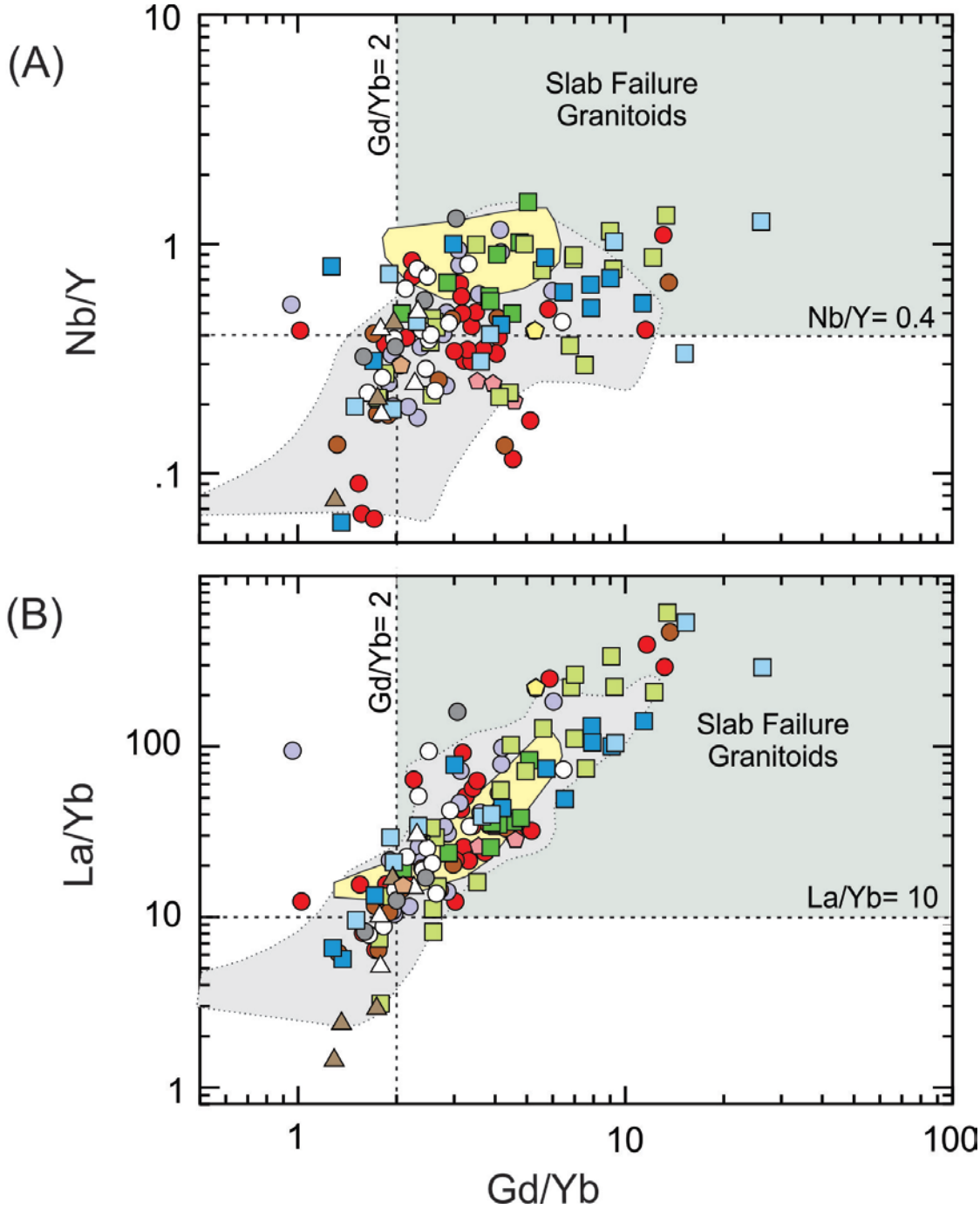

Figure 15. Paleoproterozoic Thelon tectonic zone igneous rock samples plotted on Gd/Yb vs (a) Nb/Y, and (b) La/Yb slab-failure (SF) vs arc magmatism discrimination plots of Hildebrand and Whalen (in press). Symbols legend shown in Fig. 3 and shaded fields as in Fig. 4.

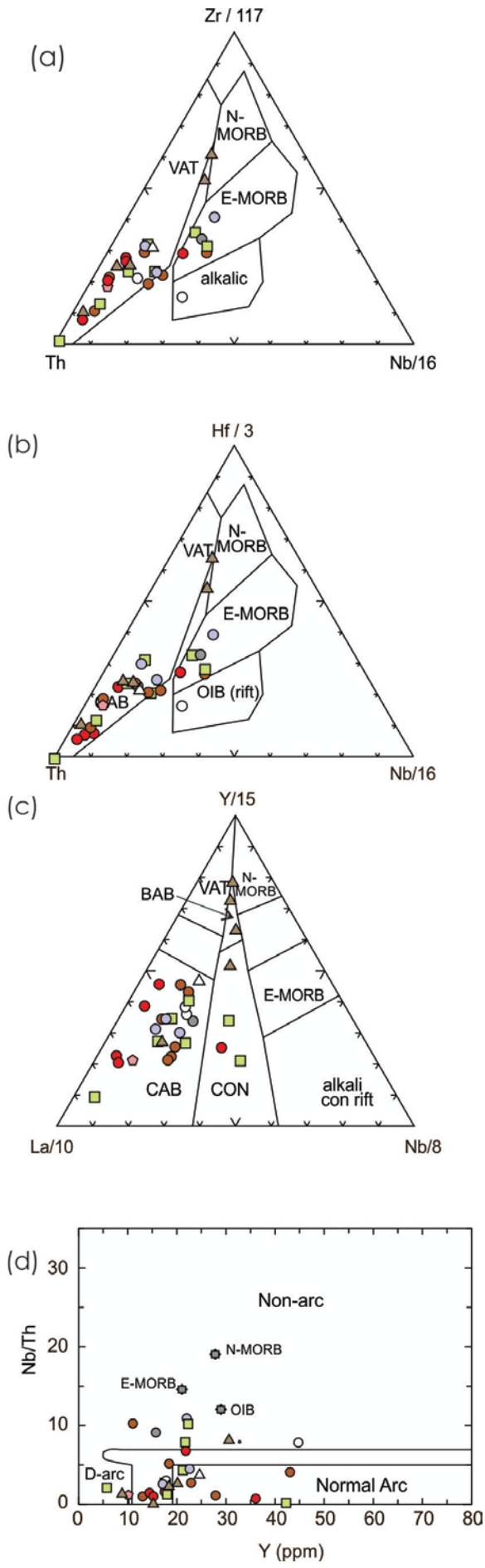

Figure 16. Paleoproterozoic Thelon tectonic zone mafic (SiO_2 <55 wt.%) igneous rock samples plotted on selected tectonic discrimination plots including; (a) Th-Zr-Nb, and (b) Th-Hf-Nb of Wood (1980); (c) La-Y-Nb of Cabinis and Lecolle (1989); and (d) Nb/Th-Y plot (after Swinden et al., 1989). Abbreviations: CAB – calc-alkaline basalt, VAT – volcanic arc tholeiite, N- and E-MORB – normal and enriched mid-ocean-ridge basalt, alkalic – alkali-basalt, BAB – back-arc basin basalt, CON – continental tholeiite, D-arc – depleted arc and OIB – ocean island basalt. Representative non-arc oceanic basalt compositions shown in (d) are from Sun and McDonough (1989).

2. *1.93-1.89 Ga TTZ granitoid groups/suites*

(a) *High-Zr granitoids* show clear affinity to post-collisional granites, plotting in the within-plate granite (WPG) field and at the boundary with the volcanic arc (VAG)field (Fig. 13a). On the Nb vs Y plot, high Zr granites plot in the WPG field, whereas on the Ta vs Yb plot, this suite plots both within the SF and WPG fields (Figs. 13b,c). Also, this suite displays SF signatures for all trace element ratios except Sr/Y, a ratio which is sensitive to late fluid-related alteration (Hildebrand and Whalen, 2017; Figs. 14, 15).

(b) *Normal-Zr granitoids (without garnet)* plot largely within the VAG and post-COLG fields (Fig. 13a) with one mafic sample being highly depleted in Rb. On Nb vs Y and Ta vs Yb plots, samples plot either in the SF (n=12) or arc (n=8) fields (Figs. 13b,c). On SF trace element ratio plots, normal Zr granitoids mainly display SF-like signatures for La/Yb and Gd/Yb, but not Nb/Y or Sr/Y, for which samples display both high (SF-like) and lower values (Figs. 14,15). These 'mixed' SF vs arc signatures within suites or groups will be discussed further below. Four of the six <55% SiO_2 samples possess normal arc signatures, whereas two are non arc-like (E-MORB or continental tholeiite; Fig. 16).

(d) *Garnet leucogranites of the main belt and west* plot almost exclusively in the syn-collisional granite field (Fig. 13a), whereas on Nb vs Y and Ta vs Yb plots (Figs. 13b,c) this peraluminous suite plots almost exclusively in the SF field. These samples display elevated trace element SF ratio values for Nb/Y, La/Yb and Gd/Yb but not Sr/Y (Figs. 14 and 15).

(e) *Eastern garnet leucogranite samples* plot both within the syn-COLG and post-COLG fields (Fig. 13a) and on Nb vs Y and Ta vs Yb plots the group splits about evenly between SF and arc fields (Figs. 13b,c). On SF ratio plots (Figs. 14 and 15) this group exhibits both high and low Nb/Y values, mainly high La/Yb and Gd/Yb and mainly low Sr/Y values.

3. *Ellice River domain volcanic and hypabyssal intrusive rocks.*

The Ellice River volcanic and hypabyssal intrusive rocks plot both in the arc and slab failure fields on Fig. 13b,c, and exhibit mainly low, arc-like, SF ratio values in Figs. 14 and 15. On mafic rock discrimination diagrams, the samples are split between arc-like (CAB and VAT) and non-arc (MORB) signatures on Nb- and Th-related plots (Fig. 16a, b, d), but four of the five samples plot in the back arc basin field on the La-Nb-Y plot (Fig. 16c). The one sample (S044) that plots in the arc field on all mafic rock diagrams (Fig. 16) has the most depleted spidergram pattern (Fig. 11d). The similarity of these geochemical characteristics to Ellice River domain hypabyssal intrusives, one of which is dated at 1955 Ma (sample M32), suggests that it may be similar in age. We consider that the other four volcanic rocks may have formed in a contemporaneous back arc basin (Fig. 16c) or they may be ca. 2.2 – 2.1 Ga, similar in age to mafic dykes recognized in the Rae (Davis et al., 2006).

Discussion:

Characteristics of TTZ basement domains

The TTZ is situated between the Rae craton on the east and Slave craton on the west (Fig. 1). In this study, Archean basement rocks that border, and may potentially form the substrate to the TTZ, are subdivided into four geographic domains. Geochemical contrasts between three of these domains (Slave-YSg, Overby, Rae) are well defined by the data outlined above, and support their interpretation as distinct crustal blocks. Although the western Rae craton (QMb) and Slave-Overby domains have similar whole rock geochemistry (e.g., medium-K), unpublished Nd isotopic data (Berman et al., 2016; 2017) and U-Pb zircon ages demonstrate that the western Rae craton (Queen Maud block) is considerably older (Tersmette, 2012; Davis et al., 2014). The Overby Lake domain is distinguished from the Slave-YSg domain in its lower K_2O, metaluminous geochemistry and slightly older Nd model ages (Berman et al., 2016; 2017).

The presence of Archean gneiss in the Ellice River domain is constrained by only one locality (L3), which limits geochemical comparisons. A further complication is that gneissic sample L3 appears to consist of two lithologies: a ca. 2.6 Ga intermediate, low-K plutonic host rock and Proterozoic, more felsic, high-K veins. This interpretation allows that sample L3 is representative of Slave-Overby Lake crust, and is supported by similar Nd model ages of L3 and Overby Lake samples (Berman et al., 2016; 2017).

Tectonic Setting of TTZ

Two markedly contrasting tectonic models have been proposed for the TTZ: (1) an intracontinental mountain belt that formed far removed from an active plate boundary; this model was first suggested by Thompson (1989) based on metamorphic constraints; it has also been proposed by Schultz et al. (2007), based on the TMZ model of Chacko et al. (2000) and De et al. (2000) and the assumption that the TTZ and TMZ are correlative; and (2) a continental margin arc formed on the edge of the Rae craton prior to continent-continent (Slave-Rae) collision (Hoffman, 1988; Culshaw et al., 1991). If the first model is valid, Paleoproterozoic TTZ igneous rocks should reflect crustal recycling, likely facilitated by mantle-derived heat, with no evidence for the involvement of destructive margin processes. If the second model is valid, the TTZ is predicted to contain at least some of the following tectonostratigraphic elements: (a) oceanic remnants, such as ophiolitic MORB-like rocks or ocean island OIB-like rocks; (b) arc-type volcanic and plutonic rocks that record destructive margin activity prior to collision; and (c) post-collisional ± slab-failure (SF) related volcanic and plutonic rocks (cf. Hildebrand and Whalen, 2015, 2017).

Geochemical data presented above does not support the presence of MORB-type oceanic rocks in the TTZ (cf. Fig. 16). However, the trace element signatures of ca. 2.07-1.96 Ga TTZ plutonic rocks point to their formation in a convergent margin tectonic setting (Fig. 13a-c), with the analyzed samples (n=72) approximately split between the arc and SF fields (Figs. 13b, c).

Although trace element signatures can to some extent be inherited from source rocks (Tarney and Jones, 1994; Hawkesworth et al., 1995; Hooper et al., 2000, Chacko et al., 2000), the major element chemistry of the TTZ sample suite also supports a convergent margin tectonic setting. In Phanerozoic & Paleoproterozoic subduction zones, mafic compositions comprise >30% of plutonic suites in arcs, but <10% in intracratonic settings (Chacko et al., 2000; Driver et al., 2000). In the TTZ suite, > 40% of analyzed TTZ plutonic rocks have mafic compositions (fields 3a, 7, 8, 13-15 on Fig 4). This significant mafic component of TTZ plutonism is also inconsistent with their formation dominantly via slab failure, as most SF suites are characterized by plutonic rocks in the 60-70% SiO_2 range with very few mafic compositions (Hildebrand and Whalen, 2017). This observation suggests that most TTZ mafic rocks represent arc plutons, a conclusion supported by the observation that 8 of 10 mafic rocks with normative quartz >5% (as used in Pearce et al.'s (1984) geochemical discriminations) plot in the arc field on the Nb vs. Y tectonic discrimination plot (red outline in Fig. 16b). More felsic compositions likely reflect both arc and SF plutonism, although 2.07-2.02 Ga samples plot in or on the boundary of the arc field as expected for the oldest plutonic rocks. It is important to recognize SF plutons because of the potential insight they yield on the timing of collisional events (each of which is followed by slab failure), but distinguishing between arc and SF plutonism can be challenging. In a convergent margin setting, understanding of field relationships, including intrusive contacts and deformation fabrics are required to distinguish effectively pre-collisional arc suites from post-collisional ± slab failure (SF) suites, which may be only separated by 2 to 5 Myr (Hildebrand and Whalen, 2015, 2017). In the TTZ, syn- to late-tectonic penetrative deformation has overprinted and obscured such field relationships, such that, in the absence of much more detailed U-Pb geochronology, their geochemical signatures remain as the main means of separating pre- and syn-collisional (arc-like) suites from later post-collisional ± slab failure suites. An additional impediment to tectonic understanding is the degree to which plutonic rock SF ratios are modified by interaction with basement and its cover, as discussed further below.

'Adakitic' and 'Slab Failure' Signatures

Archean sodic granitoids, usually termed the TTG (tonalite–trondhjemite–granodiorite) series or suite, are a volumetrically predominate component of Archean cratons (e.g. Martin, 1994). TTG suites display distinctive high La/Yb and Sr/Y values, termed the 'adakitic signature' (Moyen, 2009) and attributed to partial melting of mafic protoliths, with elevated La/Yb reflecting residual garnet, a HREE-enriched mineral, and high Sr/Y reflecting both instability of plagioclase, a Sr-enriched mineral, and stability of garnet, a Y-rich mineral. The 'adakitic signature' is reflected in both Archean Rae and Slave rocks that border, and possibly underlie the TTZ (see Figs. 14, 15).

Hildebrand and Whalen (2015, 2017) have documented that adakitic Sr/Y signatures, ***plus*** elevated Nb/Yb and Gd/Yb, are characteristic of SF-related magmatism in the North American Cordillera. Further, they proposed SF plutonism represents as much as 80% of exposed NA Cordilleran batholithic rocks, and that SF plutonism in the NA Cordillera typically follows arc

plutonism by <10 Myr. The presence in ca. 2.06-1.96 Ga TTZ rocks of some adakitic geochemical characteristics, as described and illustrated above (Figs. 14, 15), suggests that SF processes may have played a role in the petrogenesis of some of these rocks. Relevant to this discussion is that La/Yb, Gd/Yb and Sr/Y values within Cordilleran slab-failure related plutonic suites are between 10 - 100, 2 - 10 and 20 - 400, respectively (Hildebrand and Whalen, 2017). In contrast, numerous Paleoproterozoic TTZ plutonic samples, exhibit La/Yb>100, some have Gd/Yb>10, and some 50% have Sr/Y<20 (Figs. 14 and 15), i.e., the HREE garnet-related signatures are magnified and the Sr plagioclase-related signature is muted.

In order to assess whether a SF mechanism is relevant for TTZ magmatism, a first order question that needs to be determined is whether components of SF signatures could have been 'recycled' or 'remagmatised' via partial melting of TTZ Archean basement rocks, given the presence of similar geochemical signatures within older rocks that border and likely form the deeper crustal substrate to TTZ, along with Nd isotopic data indicative of interaction of Paleoproterozoic plutonic suites with old basement (Berman et al., 2016, 2017). In other words, to what extent does the trace element geochemistry of Paleoproterozoic TTZ plutons actually reflect Paleoproterozoic tectonomagmatic processes? Exposed Mesoarchean igneous basement rocks are mainly tonalitic to granitic in composition (Fig. 4a) and contain >20 vol% plagioclase. In general, partial melting of such protoliths would almost invariably leave residual Sr-enriched plagioclase, such that the high Sr/Y signature of the protolith would probably not be 'recycled' into derived partial melts. In contrast, unless there was a LREE-enriched residual mineral, it is likely that the HREE-depleted (high La/Yb and Gd/Yb) signature of the basement rocks would also be a feature of derived partial melts. However, the likely Archean basement rocks to the TTZ are relatively anhydrous igneous rocks that underwent high-grade metamorphism during the Arrowsmith orogeny at ca. 2.35 Ga (Berman et al., 2013; Davis et al., 2013; 2014), and thus are not fertile protoliths for generating the significant volumes of partial melt required to form the voluminous metaluminous to slightly peraluminous (Fig. 8b; i.e., I-type) early TTZ plutonic suites.

An alternative to the 'remagmatization' petrogenetic model, is that the low Sr/Y values of many 60-70 wt.% SiO_2 range plutonic rocks, particularly the early metaluminous TTZ plutonic groups, reflect a combination of AFC (assimilation-fractional-crystallization) (cf. DePaolo, 1981) and MASH (melting, assimilation, storage and homogenization) (cf. Hildereth and Moorbath, 1988) processes. In this model, upper mantle-derived high temperature magmas with distinctive slab failure high-pressure trace element signatures pond within TTG-dominated Archean basement, simultaneously assimilating crustal components, mixing and fractionating a mineral assemblage dominated by plagioclase. This combination of processes would decrease or remove the original plagioclase-related high Sr content and high Sr/Y signature of the magmas, while assimilation of Archean crust with SF characteristics would magnify the garnet-related trace element ratios (La/Yb, Gd/Yb and Sm/Yb), and to a lesser extent the ratios related to garnet and ilmenite/rutile (Nb/Y and Ta/Yb). Related to the above AFC and MASH discussion is that

assimilation of sedimentary rocks which have similarly elevated SF ratios as Rae craton basement, provides an additional means to increase SF ratios of plutonic rocks (arc or SF). Evidence for this process being operative can be seen in a general, but not perfect correlation, between elevated SF ratios and higher $\delta^{18}O$ (Taylor et al., unpublished data). As is the case for interaction with igneous basement rocks, Sr/Y ratios could be boosted or lowered depending on whether the sedimentary rocks were plagioclase poor or rich enough to leave residual plagioclase.

It should be noted that the 1.9 Ga leucogranite suite shows high Nb/Y, La/Yb and Gd/Yb, but low Sr/Y (medium blue squares in Fig. 14). Peraluminous compositions and high $\delta^{18}O$ isotopic signatures (Taylor et al., 2017) indicate generation of TTZ leucogranites during ca. 1.9 Ga high grade metamorphism and melting of a sedimentary basin off the west flank of the Rae craton. As experimental studies demonstrate that garnet is a ubiquitous, peritectic product of melting metapelitic rocks (e.g. Patino-Douce and Johnson, 1991; Vielzeuf and Montel, 1994), partial melting of TTZ sedimentary protoliths at moderate pressures where garnet and plagioclase are stable phases accounts for the high SF-like garnet ratios accompanied by low Sr/Y.

The normal-Zr, ca. 1.9 Ga plutonic suite is interpreted to have acquired its mixed arc-like and SF-like signatures via interaction with Mesoarchean crust with SF geochemical characteristics at relatively low pressure during the high-grade, ca. 1.9 Ga regional metamorphism that is well documented across all domains (Mitchell et al., 2017). This model is probably not, however, applicable to the ca. 1.9 Ga post-collisional rocks. Genesis of the distinctive high-Zr alkaline (A-type) suite, characterized by Sr/Y<20 but high La/Yb and Gd/Yb signatures (Fig. 14), likely requires input from enriched subcontinental lithospheric mantle sources, not just crustal materials, a common occurrence in post-collisional settings (cf. Whalen et al., 2006).

In general, the geochemistry of Paleproterozoic TTZ igneous rocks suggests that SF-type geochemical characteristics may be almost as abundant in the TTZ as arc-like rocks. Although the degree of “SF inheritance” from Archean protoliths still needs to be determined, this can also be explained by significant uplift and erosion of the upper plate during slab failure, during which, depending on the location of the suture, previously abundant arc rocks can be exhumed (Hildebrand and Whalen, 2015, 2017), leaving SF rocks as the main magmatic record of a former destructive margin. It is important to note that, along with identifying the 'adakitic-like', post-collisional slab failure (SF) origin of a large proportion of NA Cordilleran orogenic belt magmatism, Hildebrand and Whalen (2015, 2017) recognized that SF plutonic rocks can be progenitors to economically significant mineralization. Although post-collision uplift may have removed most high-level sub-volcanic mineralization, deep-level mineralized roots to these systems, or isolated high-level crustal domains, such as those that expose potential ca. 1.95 Ga volcanic rocks, may still be preserved in the TTZ.

The TTZ is not the first example of SF magmatism within a Paleoproterozoic orogen, as a number of linear belts of SF plutonic rocks have been previously identified within the Flin Flon Assemblage, Trans-Hudson orogen (Whalen et al., 2016). In that orogen, which evolved within an intraoceanic domain, oceanic, arc and back-arc igneous suites are all juxtaposed and preserved, such that its formation by modern-type plate tectonic processes has been long recognized (Lucas et al., 1996 and references therein). In this segment of the Trans-Hudson orogen, the accreted components were all initially underlain by juvenile thin crust, such that collisions followed by slab failure did not result in major uplift and erosion of earlier arc-related magmatic rocks, as may have occurred within the TTZ.

Comparison of TMZ and TTZ Plutonic Rocks

Geological background of Taltson magmatic zone

The large scale geology of the TMZ exposed in northern Alberta and southern Northwest Territories (Fig. 1), is fairly well constrained from regional mapping and supporting isotopic and geochemical studies (Godfrey, 1986; Baadsgaard and Godfrey, 1967; Goff et al., 1986; Bostock et al., 1987, 1991; McDonough et al., 2000; McNichol et al., 2000; Chacko et al., 2000; De et al., 2000). The TMZ comprises 1.99 – 1.93 Ga granitoid rocks that can be divided into two age groups. The older group consists of 1.99 – 1.96 Ga hornblende-biotite, metaluminous to slightly peraluminous granites which comprise the eastern TMZ in northern Saskatchewan (Wyllie Lake, Colin Lake suites) but the western TMZ in the Northwest Territories (Deskanalata). The younger group consists of 1.95 – 1.93 Ga peraluminous granites (Slave, Konth, Arch Lake suites) which contain numerous enclaves of high-grade metapelite, interpreted as the remnants of the once continuous 2.17 – 2.04 Ga Rutledge River sedimentary basin (Bostock and van Breemen, 1994). Both groups of granitoids intrude the Taltson basement complex, which consists dominantly of ca. 3.2–2.9 Ga gneisses intruded by 2.4 – 2.2 Ga granitoids. The presence of Mesoarchean rocks in the Taltson basement complex leaves open the possibility that it was originally connected with the Queen Maud block further north, such that Mesoarchean crust formed a continuous domain on the western flank of the Rae craton prior to 2.0-1.9 Ga orogenesis.

TMZ Plutonic Basement

Published geochemical data from basement gneisses of the TMZ from Goff et al. (1986) and De et al. (2000) are from samples without geochronological control. These data are plotted on the same geochemical plots employed above for TTZ plutonic rocks in Figs. 17a to 24. Compared to Archean basement rocks adjacent to, or east of, the TTZ (i.e., Queen Maud block, Rae craton), TMZ basement gneisses are notably more felsic, being predominated by high-K to shoshonitic alkali-feldspar granites and syenogranites, and consist of slightly to strongly peraluminous (ASI>1.1) compositions (Fig. 21a). As well, TMZ basement gneisses plot almost exclusively at the minimum melt end-point area of alkalic to calcic trends (Fig. 17a, 20a).

TMZ basement rocks plot almost exclusively in the post-collisional granite field with some overlap into the syn-COLG field (Fig. 22a), but some plot in the adjacent WPG field.. They show strong slab failure (SF) affinity, generally exhibiting Nb/Y values >0.4, La/Yb >10 and Gd/Yb >2, a distinguishing feature of SF rocks, but almost all exhibit a non-SF-like large range in Sr/Y values (Fig. 23). However, due to their exclusively felsic peraluminous character, the trace elements signatures of TMZ basement rocks likely reflect derivation from, or major input from, garnet-bearing metasedimentary materials, not high P-T mafic protoliths, i.e. these rocks are likely not SF related. None of the Archean basement domains in the TTZ exhibit much overlap with the TMZ basement gneisses in terms of trace element ratios (Figure 22 and 23), as would be expected if they were derived from distinctly different protoliths and P-T conditions.

The above geochemical data indicate that Paleoproterozoic TMZ plutonic suites are dominantly not underlain by the distinctive, low-K plutonic rocks exposed in the QMb. Although we cannot rule out along strike compositional differences in Mesoarchean Rae basement, this geochemical difference is not surprising given the abundance of ca. 2.4-2.3 Ga plutonic rocks that have intruded Mesoarchean basement in the TMZ (Bostock et al., 1987, 1991; McNichol et al., 2000). In the TTZ there is only one locality on the western flank of the Duggan Lake domain (QMb) that has thus far yielded a crystallization age of ca. 2.4 Ga (sample N026c).

Paleoproterozoic Plutonic Suites

Published geochemical data for Paleoproterozoic TMZ early ca. 1.99-1.96 Ga and late ca. 1.95-1.93 Ga plutonic suites (Goff et al., 1986); Theriault, 1990; De et al., 2000) are compared to Paleoproterozoic TTZ plutonic rocks in Figs. 17b to 24. The older plutonic suite exhibits a broad compositional range from alkali-feldspar granite through granodiorite to quartz diorite (Fig. 17b). This range is similar to older (2.06-1.99 Ga) TTZ plutonic units (Fig. 4b), except that the latter includes a significant population of more mafic rocks (quartz diorite, diorite, gabbro). The younger TMZ plutonic suite is dominated by alkali-feldspar granites, syenogranites and monzogranite, similar to younger (ca 1.9 Ga) TTZ plutonic units. The older TMZ and TTZ rocks exhibit a similar large range in SiO_2 and K_2O contents (Figs. 5b and 18b), whereas the younger TMZ and TTZ suites consist mostly of felsic high-K to shoshonitic compositions. Most Paleoproterozoic TMZ plutonic rocks are magnesian and range to quite low Fe* values (Fig. 19b). In contrast, older TTZ plutonic units are almost all magnesian, whereas younger TTZ units include both ferroan and magnesian samples (Fig. 6b). Both older TMZ and TTZ suites are dominantly calc-alkalic to alkalic (Figs. 7b and 18b) but older TTZ units range to lower ASI values than the older TMZ suite (Figs. 8b and 21b). In contrast, the younger TMZ suite is almost exclusively peraluminous, with ASI values >1.1 predominating, whereas younger TTZ plutonic units include both metaluminous and strongly peraluminous samples (Fig. 8b and 21b).

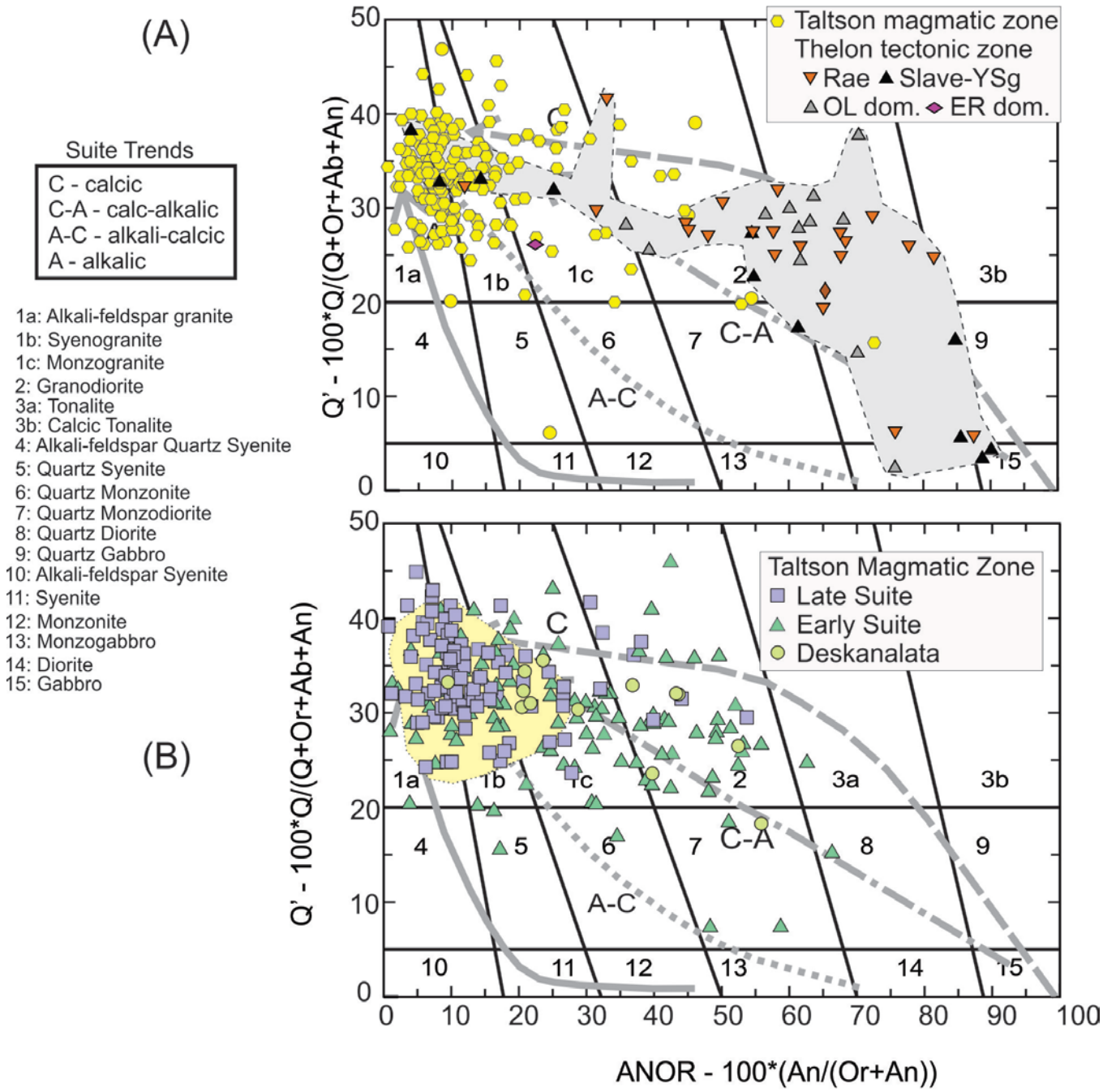

Figure 17. Taltson magmatic zone: (a) Archean basement rocks; and (b) Paleoproterozoic plutonic rocks plotted on the normative Q' versus ANOR classification plot. Data from Goff et al. (1986), De et al. (2000) and Theriault (1990). Fields and references as in Fig. 4.

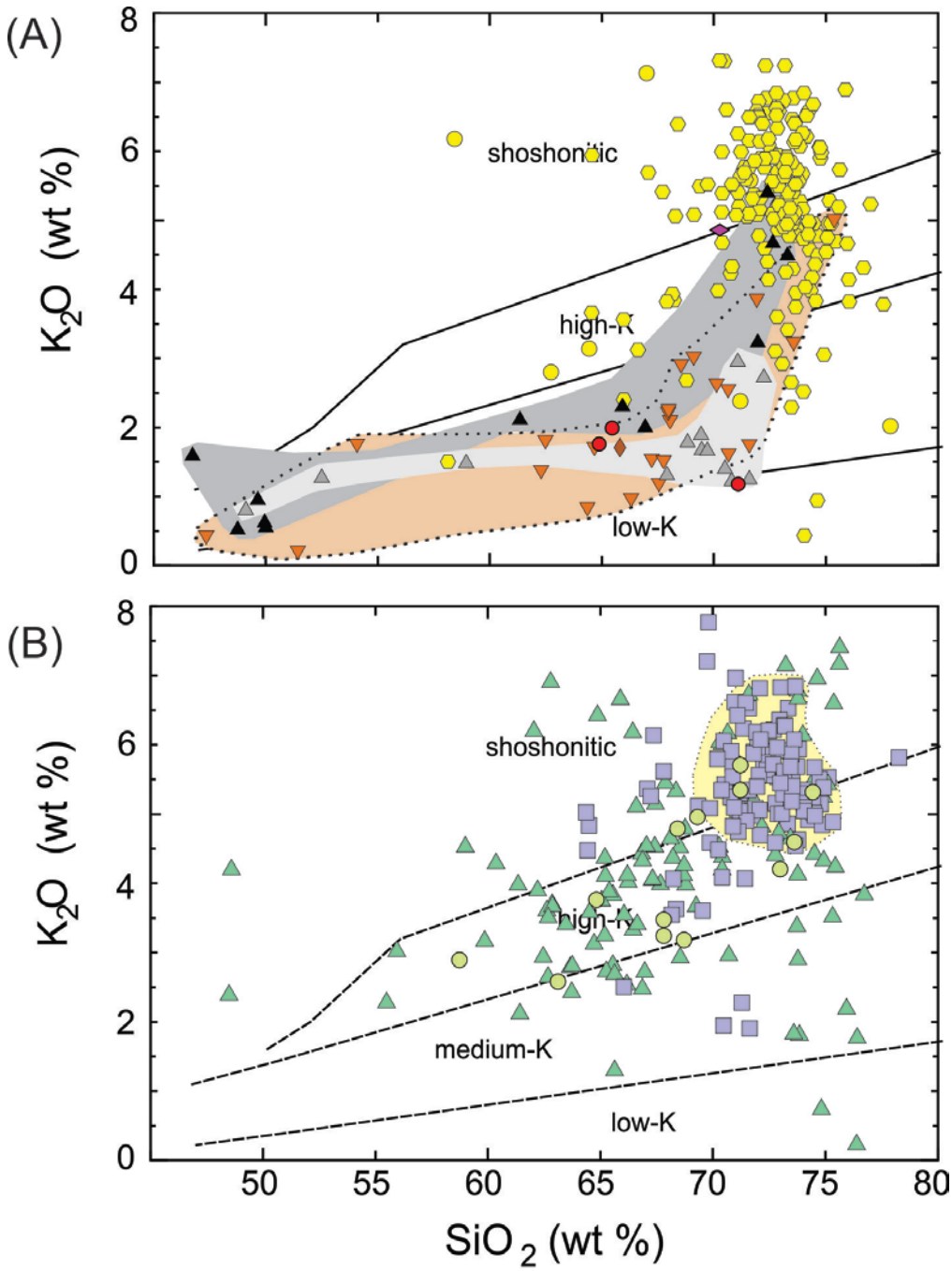

Figure 18. Taltson magmatic zone: (a) Archean basement rocks; and (b) Paleoproterozoic plutonic rocks plotted on a SiO_2 vs. K_2O plot. References and fields as in Figs. 5 and 17.

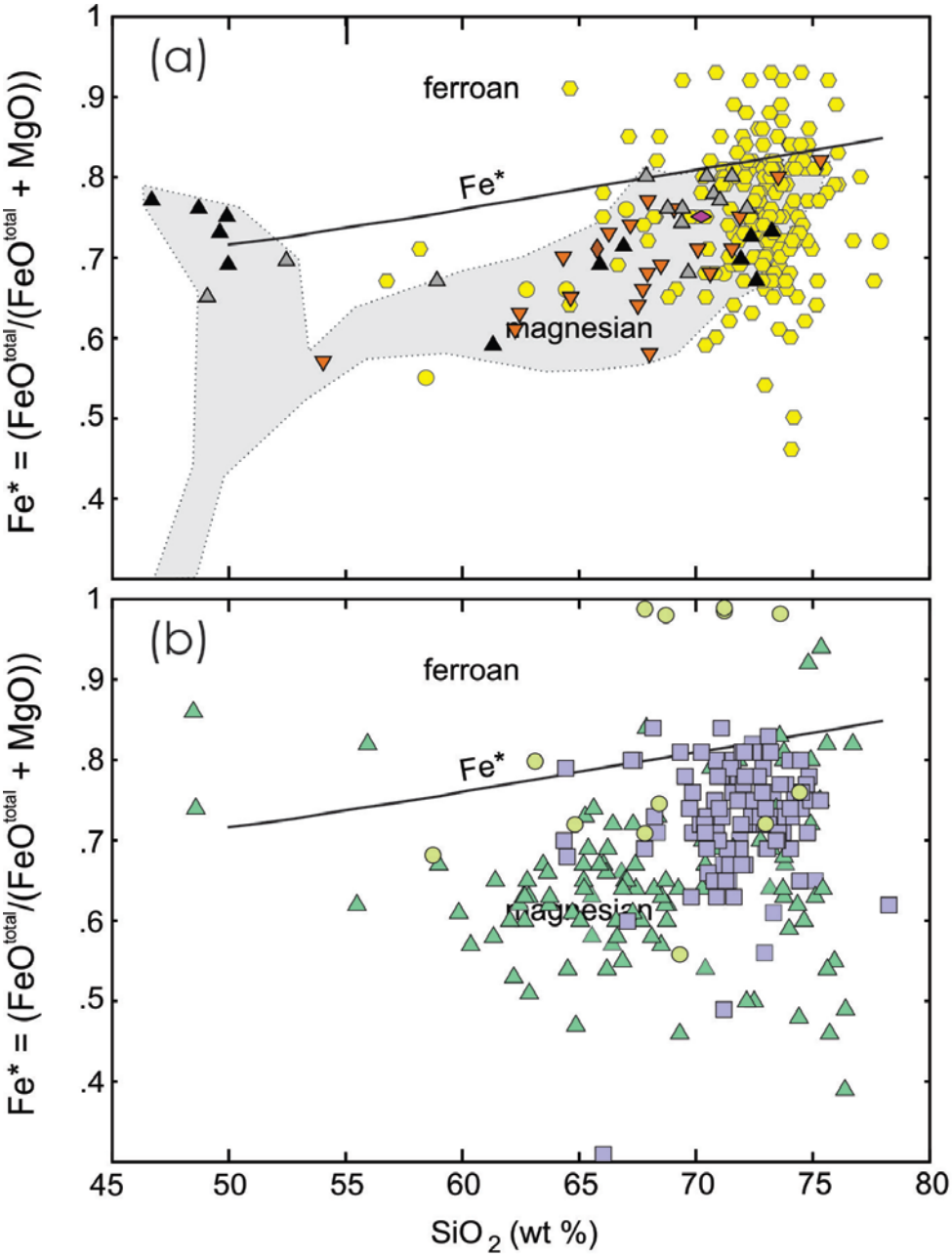

Figure 19. Taltson magmatic zone: (a) Archean basement rocks; and (b) Paleoproterozoic plutonic rocks plotted on the $FeO^{total}/(FeO^{total} + MgO)$ (or Fe*) vs. SiO_2 granitic rock classification plot; references and fields as in Figs. 6 and 17.

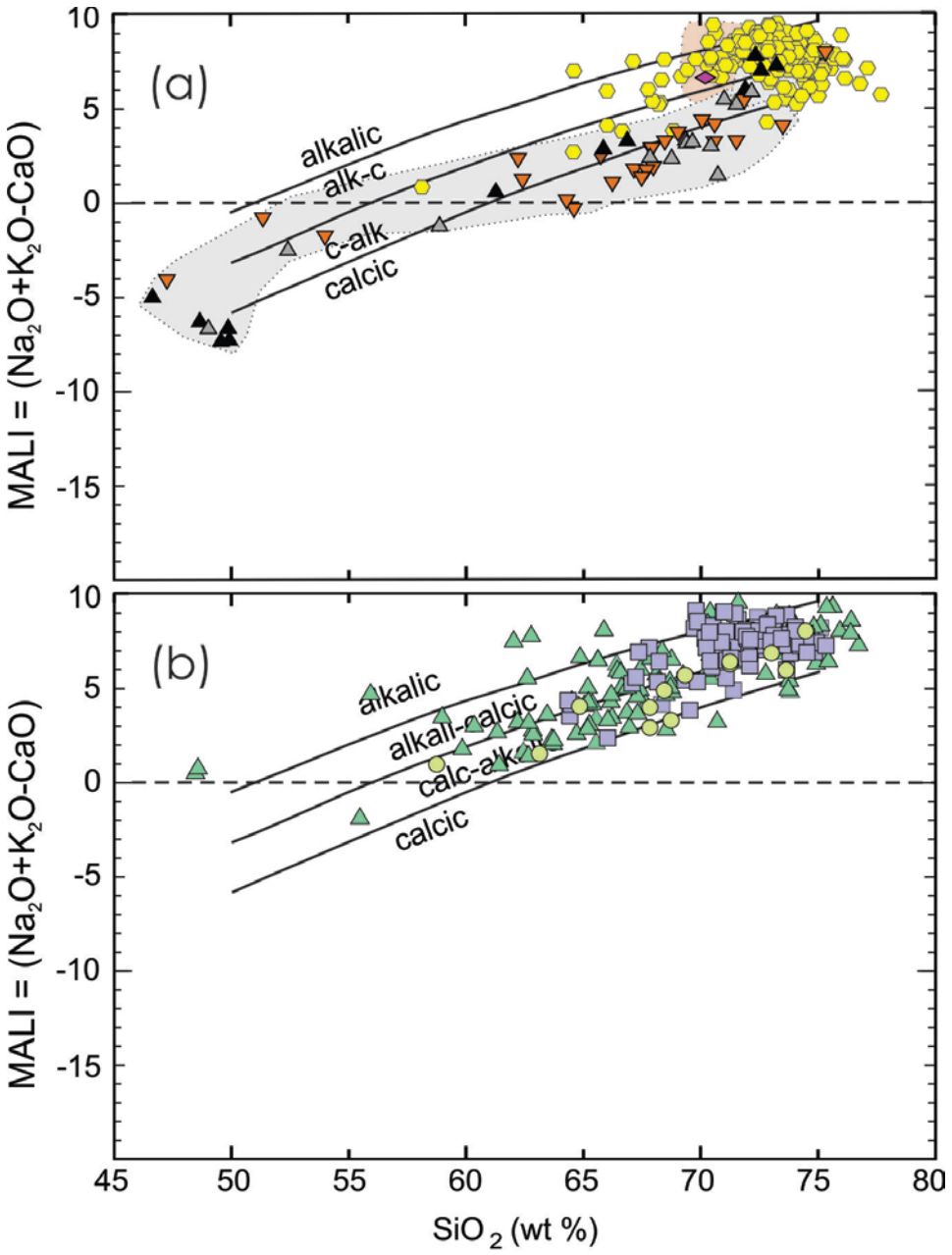

Figure 20. Taltson magmatic zone: (a) Archean basement rocks; and (b) Paleoproterozoic plutonic rocks plotted on the Na_2O+K_2O-CaO (or MALI) vs. SiO_2 granitic rock classification plot; references and fields as in Figs. 6 and 17.

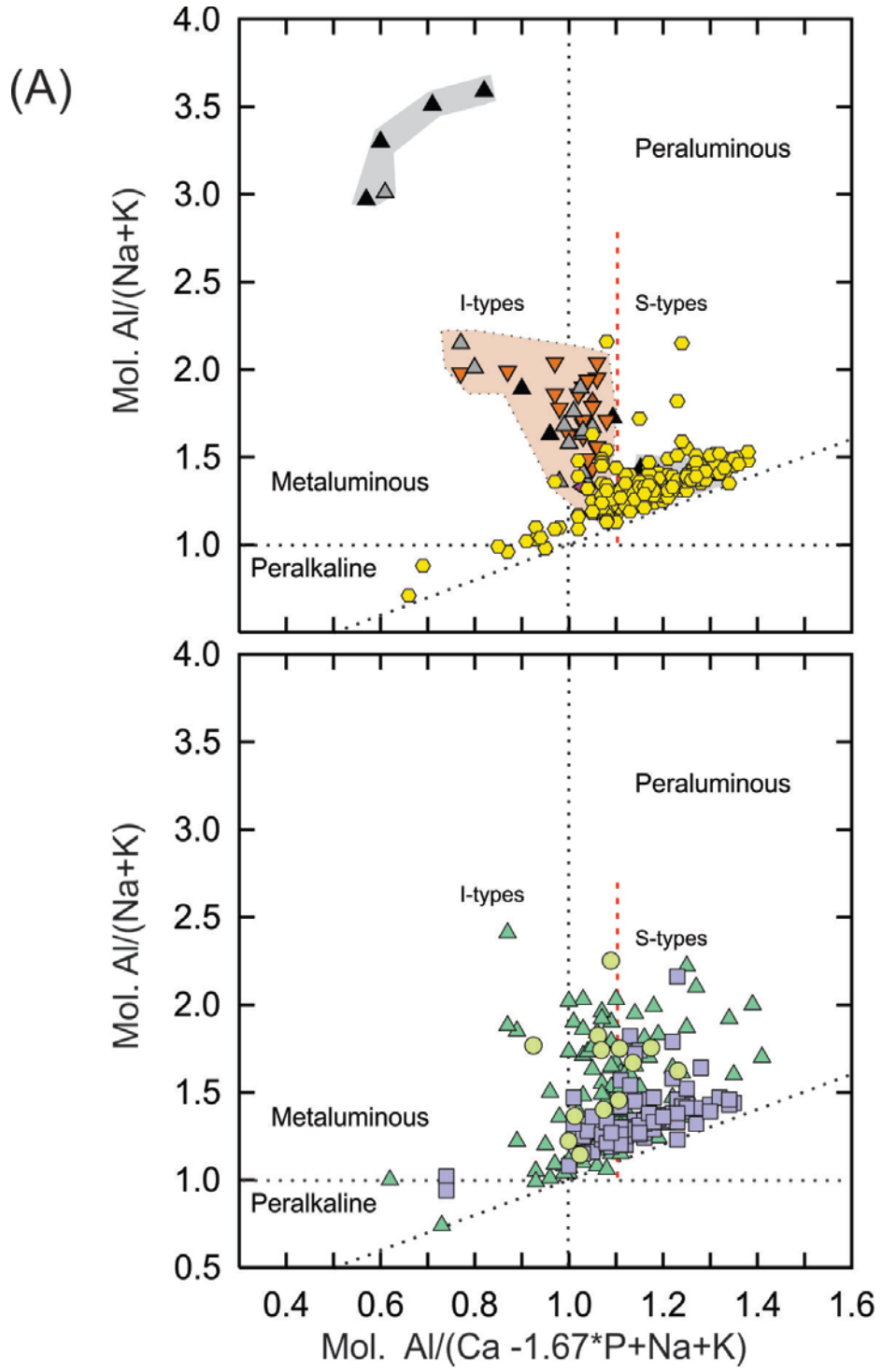

Figure 21. Taltson magmatic zone: (a) Archean basement rocks; and (b) Paleoproterozoic plutonic rocks plotted on a Shand (1943) plot of Al saturation index (molecular Al/(Ca+Na+K-1.67*P)) versus alkali saturation index (molecular Al/(Na+K)); references and fields as in Figs. 8 and 17.

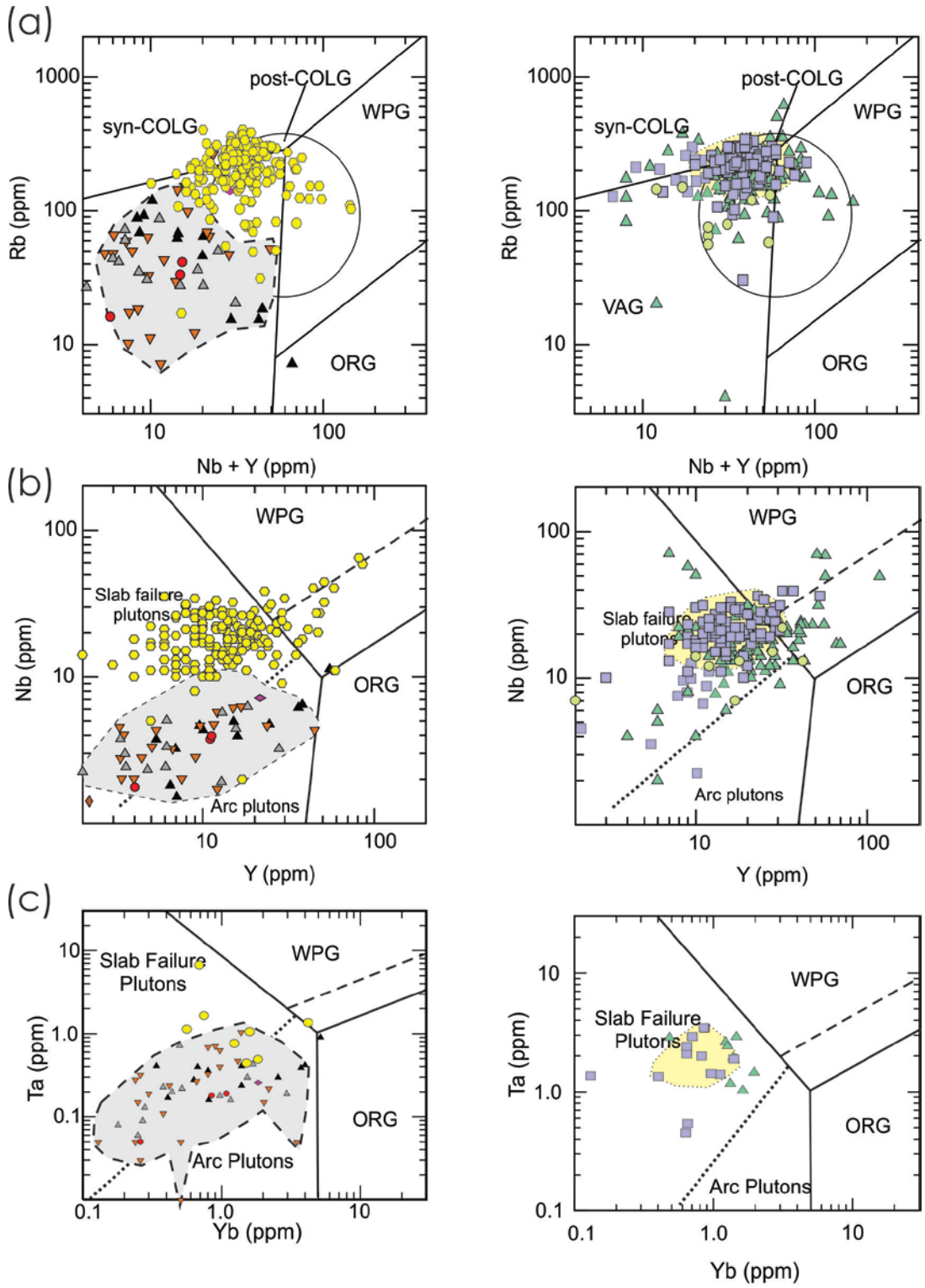

Figure 22. Taltson magmatic zone: (a) Archean basement rocks; and (b) Paleoproterozoic plutonic rocks plotted on: (a) Rb vs Y+Nb; (b) Nb vs Y; and (c) Ta vs Yb granitoid tectonomagmatic discrimination plots; references, abbreviations and fields as in Figs. 13 and 17.

Both Paleoproterozoic TMZ temporal groups plot almost exclusively in the post-COLG field, with a proportion ranging into both the syn-COLG and VAG fields (Fig. 22a). TTZ ca 2.06-1.96 Ga (Wpb, ERpb, Cpb, Epb) and ca.1.9 Ga units exhibit similar overlapping compositional ranges on this plot (Fig. 13a), but with a greater proportion plotting in the VAG field particularly with lower Rb content. Both older and younger TMZ suites plot almost exclusively in the SF fields or show dispersion into the WPG field (Figs. 22b, c), similar to ca. 1.9 Ga TTZ units (Figs. 13b, c). In contrast, ca. 2.06-1.96 Ga TTZ units are about evenly divided between the SF and arc fields without crossing into the WPG field (Figs. 13b, c). Early and late TMZ suites completely overlap and consistently exhibit high slab-failure like Nb/Y, La/Yb and Gd/Yb values (Fig. 23), but mainly Sr/Y values <20 (arc-like). In contrast, older ca. 2.06-1.96 Ga TTZ samples exhibit significant ranges in Nb/Y, La/Yb and Gd/Yb values, plotting within both the SF and arc fields (Fig. 14), whereas younger ca. 1.9 Ga TTZ samples are generally characterized by high SF-type Nb/Y, La/Yb and Gd/Yb values with Sr/Y values both <20 (arc-like) and >20 (SF-like). Although HREE data for TMZ samples are scarce, available data suggest both older and younger TMZ suites overlap, with almost all samples plotting in the SF fields (Fig. 24). In comparison, both older and younger TTZ plutonic samples yield Nb/Y values >0.4 (SF-like) and <0.4 (arc-like) (Fig. 15a), whereas almost all exhibit La/Yb values >10 (SF-like) (Fig. 15b).

In summary, although there are strong geochemical similarities between younger plutonic suites of the TMZ and TTZ, there are some significant differences between the older plutonic phases that suggest they are not along-strike equivalents. Foremost amongst these differences are the greater proportion of mafic plutonic rocks and the arc-like trace element signature of some TTZ igneous rocks, both of which are lacking in the early TMZ magmatism. Additionally, TTZ plutonism is now established to have initiated by 2060 Ma (Davis et al., 2014; W.J. Davis, unpublished data), some 70 Myr prior to the earliest dated TMZ plutonic rock (Thèriault, 1992).

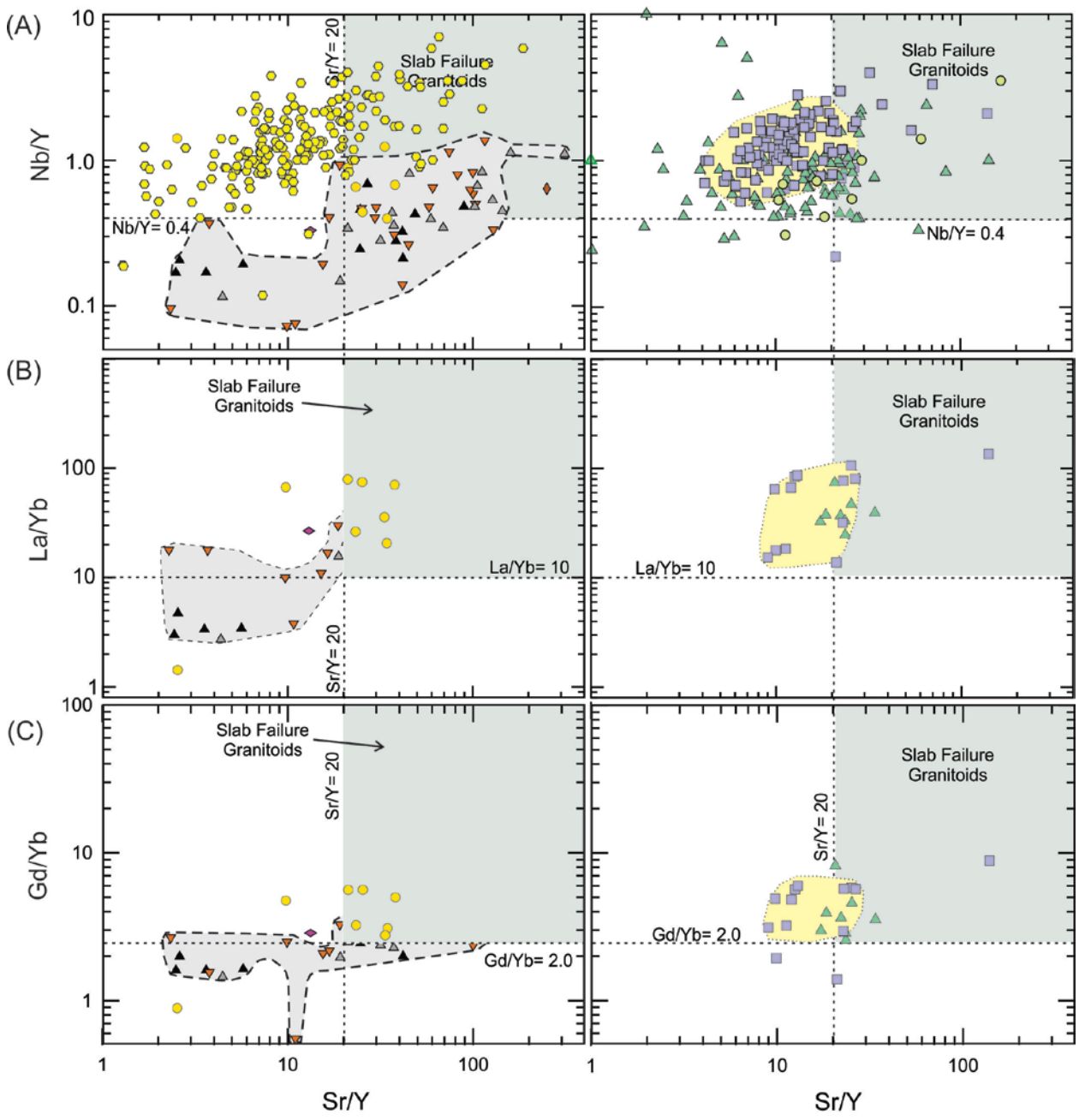

Figure 23. Taltson magmatic zone: (a) Archean basement rocks; and (b) Paleoproterozoic plutonic rocks plotted on Archean Taltson zone basement rocks plotted on Sr/Y vs (a) Nb/Y, (b) La/Yb, and (c) Gd/Yb slab-failure (SF) vs arc magmatism discrimination plots of Hildebrand and Whalen (2015); fields as in Figs. 17.

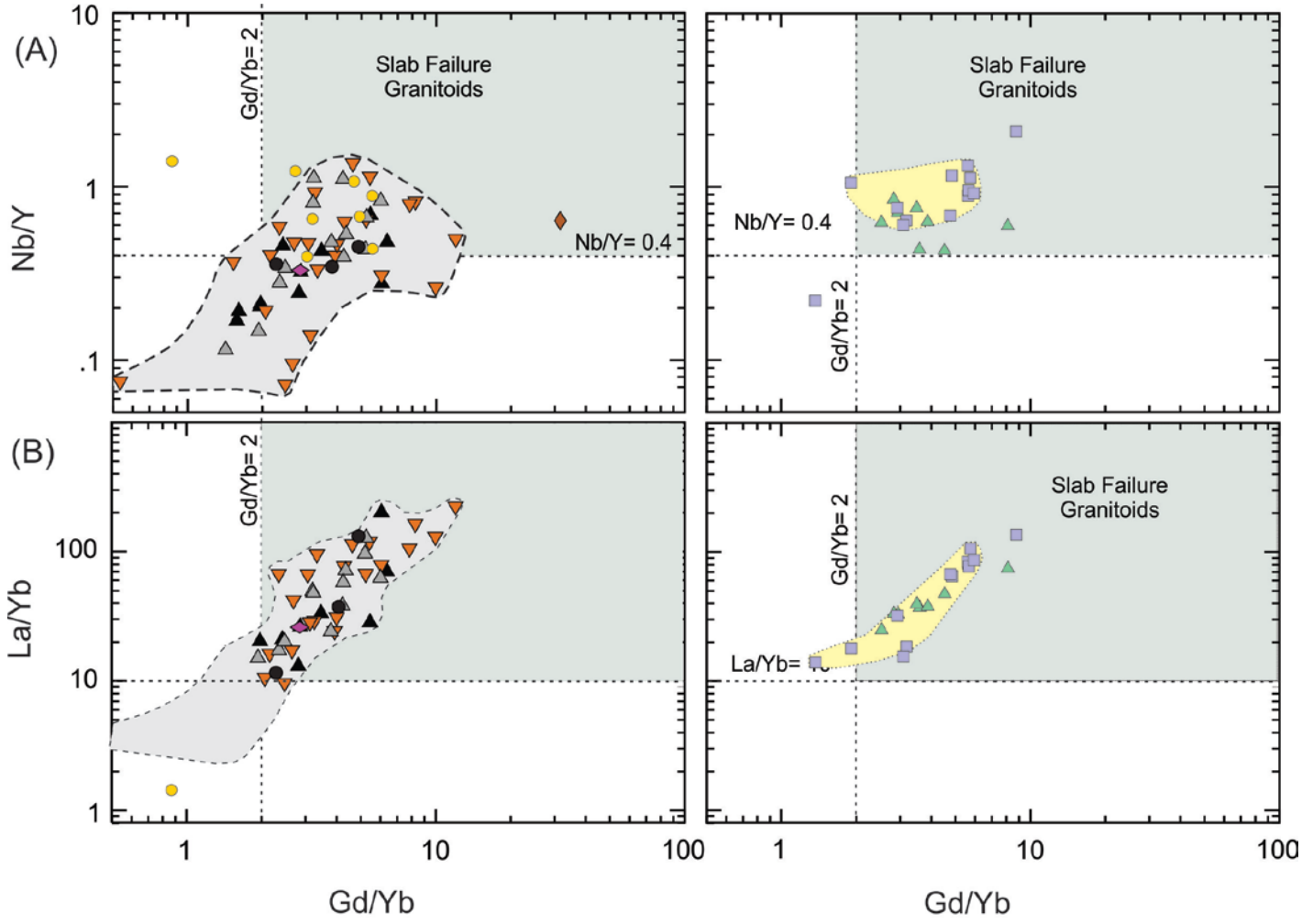

Figure 24. Taltson magmatic zone: (a) Archean basement rocks; and (b) Paleoproterozoic plutonic rocks plotted on Archean Taltson zone basement rocks plotted on Gd/Yb vs (a) Nb/Y, and (b) La/Yb slab-failure (SF) vs arc magmatism discrimination plots of Hildebrand and Whalen (in press); fields as in Fig.17.

Conclusions

The data set presented here represents the first opportunity to establish the geochemical characteristics of Thelon tectonic zone (TTZ) plutonic and volcanic rocks and address significant questions regarding the evolution of this orogenic belt along the western flank of the Rae craton. First order conclusions which can be drawn include:

- A convergent margin setting best explains the chemistry of ca. 2.07 – 1.96 Ga plutonic rocks, which display both arc and slab failure (SF) signatures.
- The majority of ca. 2.0 Ga mafic plutonic rocks are interpreted to be arc plutons, but further work is needed to distinguish arc from SF plutons in more felsic plutonic rocks.
- Distinct geochemical differences distinguish Archean plutonic rocks in the Slave-YSg, Slave-Overby Lake, Rae, and Ellice River domains.
- Geochemical comparisons indicate low-K Rae basement plutonic rocks are not a component of the TMZ basement.
- Although late (ca. 1.9 Ga) TMZ and TTZ rocks are similar geochemically, early TTZ plutonic rocks are more mafic and exhibit more arc-like signatures not present in most early TMZ plutons, suggesting that TMZ is not directly correlative with TTZ, as long assumed.
- The lack of continuity of the Taltson and Thelon orogenic belts implies that the MacDonald fault may have been an important early (≥ ca. 2.0 Ga) structure (Great Lake shear zone?) that separated these two orogenic belts and allowed them to evolve independently over different time periods.
- This study allows that the identification of SF magmatic signatures within deeply eroded Paleoproterozoic or older orogenic belts may be evidence of the operation of modern plate tectonic processes in the absence or paucity of preserved arc-type magmatic signatures.

Acknowledgements

We thank Great Slave Helicopters and Air Tindi for rotary and fixed wing air support throughout the duration of our field work, Sarah Harper for excellent meals, Bobby Klengenberg for assistance and local knowledge around camp and on traverse, Tim Chadwick, Dusty Liikane, Svieda Ma, and Michelle Caine for very capable field assistance, and Jacques Pinard for sample preparation. Neil Rogers provided a helpful, constructive review. This GSC contribution was supported by the GeoMapping for Energy and Minerals (GEM) Program.

References

Baadsgaard, H. and Godfrey, J.D., 1967. Geochronology of the Canadian Shield in northeastern Alberta; Part 1, Andrew Lake area; Canadian Journal of Earth Sciences, v. 4, p. 541-563.

Berman, R.G., Sanborn-Barrie, M., Stern, R., and Carson, C., 2005. Tectonometamorphism at ca. 2.35 and 1.85 Ga in the Rae domain, western Churchill Province, Nunavut, Canada: insights from structural, metamorphic and in situ geochronological analysis of the southwestern Committee Bay belt; Canadian Mineralogist, v. 43, p. 409-442.

Berman, R.G., Pehrsson, S., Davis, W.J., Ryan, J., Qiu, H., and Ashton, K.E., 2013. The Arrowsmith orogeny: new insights from in situ SHRIMP geochronology of the southwestern and central Rae craton; Precambrian Research, v. 232, p. 44-69.

Berman, R.G., Nadeau, L., McMartin, I., McCurdy, M., Craven, J., Girard, E., Sanborn-Barrie, M., Carr, S., Pehrsson, S., Whalen, J., Davis, W.J., Roberts, B., and Grenier, A., 2015a. Report of activities for the Geology and Mineral Potential of the Chantrey-Thelon Area: GEM-2 Thelon tectonic zone project; Geological Survey of Canada, Open File 7693, 14 p. doi:10.4095/295644

Berman, R.G., Nadeau, L., Davis, W.J., McCurdy, M., Craven, J., McMartin, I., Whalen, J., Sanborn-Barrie, M., Carr, S., Pehrsson, S., Percival, J.A., and Girard, E., 2015b. New insights into the geological evolution and economic potential of the Thelon tectonic zone and western Rae craton, Nunavut; Geological Survey of Canada, Open File 7901, 1 poster.

Berman, R.G., Sanborn-Barrie, M., Nadeau, L., Brouillette, P., Camacho, A., Davis, W.J., McCurdy, M.W., McMartin, I., Weller, O.M., Chadwick, T., Liikane, D.A., and Ma, S., 2016. Report of activities for the geology and mineral potential of the Chantrey-Thelon area: GEM-2 Rae project; GSC Open File, v. 8129, 12 p. doi:10.4095/299386

Berman, R.G., Davis, W.J., Sanborn-Barrie, M., McCurdy, M., McMartin, I., Craven, J., Roberts, B., Mitchell, R., Whalen, J., Nadeau, L., Camacho, A., Carr, S., Brouillette, P., and Girard, E., 2017. GEM-2 progress in understanding the geological evolution and economic potential of the Thelon tectonic zone; Exploration Roundup 2017, poster.

Bostock, H.H. and van Breemen, O., 1994. Ages of detrital and metamorphic zircons from a pre-Taltson magmatic zone basin at the western margin of Churchill Province; Canadian Journal of Earth Sciences, v. 31, p. 1353-1364.

Bostock, H.H., Van Breemen, O., and Loveridge, W.D., 1987. Proterozoic geochronology in the Taltson Magmatic Zone, NWT; Geological Survey of Canada, Paper, v. 87-2, p. 73-80.

Bostock, H.H., van Breemen, O., and Loveridge, W.D., 1991. Further geochronology of plutonic rocks in northern Taltson Magmatic Zone, District of Mackenzie, N.W.T. in: Geological Survey of Canada Radiometric age and isotopic studies, report 4, v. 90-2, p. 67-78.

Bowring, S.A. and Grotzinger, J.P., 1992. Implications of new chronostratigraphy for tectonic evolution of Wopmay Orogen, Northwest Canadian Shield; American Journal of Science, v. 292, p. 1-20.

Cabanis, B. and Lecolle, M., 1989. Le diagramme La/10 - Y/15 - Nb/8: un outil pour la

discrimination des series volcaniques et la mise en evidence des processus de mélange et/ou de contamination crustal. Comptes Rendus de l'Académie des Sciences Paris, v. 309, p. 2023-2029.

Chacko, T., De, S.K., Creaser, R.A., and Muehlenbachs, K., 2000. Tectonic setting of the Taltson magmatic zone at 1.9-2.0 Ga: A granitoid-based perspective; Canadian Journal of Earth Sciences, v. 37, p. 1597-1609.

Culshaw, N., 1991. Post-collisional oblique convergence along the Thelon tectonic zone, north of the Bathurst Fault, NWT, Canada; Journal of Structural Geology, v. 13, p. 501-516.

Davis, W.J. and Hegner, E., 1992. Neodymium isotopic evidence for the tectonic assembly of late Archean crust in the Slave Province, Northwest Canada; Contributions to Mineralogy and Petrology, v. 111, p. 493-504.

Davis, W., Berman, R.G., and MacKinnon, A., 2013. U-Pb Geochronology of Archival Rock Samples from the Queen Maud Block, Thelon Tectonic Zone and Rae Province, Kitikmeot Region, Nunavut, Canada; Geological Survey of Canada Open File 7409, 42 p., doi:10.4095/292663.

Davis, W.J., Berman, R.G., Nadeau, L., and Percival, J.A., 2014. U-Pb Zircon Geochronology of a Transect Across the Thelon Tectonic Zone, Queen Maud Region, and Adjacent Rae Craton, Kitikmeot Region, Nunavut, Canada. Geological Survey of Canada, Open File 7652, 38 p. doi:10.4095/295177

Davis, W., Sanborn-Barrie, M., Berman, R.G., and Pehrsson, S., 2017. U-Pb Geochronology of Paleoproterozoic supracrustal belt, Thelon tectonic zone, Nunavut; Canadian Journal of Earth Sciences (in preparation).

De, S.K., Chacko, T., Creaser, R.A., Muehlenbachs, K. 2000. Geochemical and Nd–Pb–O isotope systematics of granites from the Taltson magmatic zone, NE Alberta: implications for Early Proterozoic tectonics in western Laurentia; Precambrian Research, v. 102, p. 221–249.

DePaolo, D.J. 1981. Trace element and isotopic effects of combined wallrock assimilation and fractional crystallization; Earth and Planetary Science Letters, v. 53, p. 189–202.

Driver, L.A., Creaser, R.A., Chacko, T. and Erdmer, P., 2000. Petrogenesis of the Cretaceous Cassiar Batholith, Yukon-British Columbia, Canada: Implications for magmatism in the North American Cordilleran interior; Geological Society of America Bulletin, v. 112, p. 1119-1133.

Drummond, M.S., Defant, M.J., and Kepezhinskas, P.K., 1996. Petrogenesis of slab-derived trondhjemite-tonalite-dacite/adakite magmas; Transactions of the Royal Society of Edinburgh: Earth Sciences, v. 87, p. 205–215.

Fraser, J.A., 1964. Geological Notes On northeastern District of Mackenzie, Northwest Territories; Geological Survey of Canada, v. 63-40, p. 16 p. (inc. Map 45-1963).

Frith, R.A., 1982. Geology, Beechey Lake-Duggan Lake, District of Mackenzie; Geological Survey of Canada, Open File 851, Map, scale 1:125 000.

Frith, R.A., and van Breemen, O., 1990. U-Pb zircon age from the Himag plutonic suite, Thelon Tectonic Zone, Churchill Structural Province, Northwest Territories; Geological Survey of Canada, Paper 89-2, p. 49-54.

Frost, B.R., Barnes, C.G., Collins, W.J., Arculus, R.J., Ellis, D.J., and Frost, C.D., 2001. A geochemical classification for granitic rocks: Journal of Petrology, v. 42, p. 2033-2048.

Frost, B.R. and Frost, C.D., 2008. A geochemical classification for feldspathic igneous rocks. Journal of Petrology, v. 49, p. 1955-1969.

Godfrey, J.D., 1986. Geology of the Precambrian Shield in northeastern Alberta; Alberta Research Council, Map, v. 1986-1 (scale 1:250 000).

Goff, S.P., Godfrey, J.D., and Holland, J.G., 1986. Petrology and Geochemistry of the Canadian Shield of Northeastern Alberta; Alberta Research Council, Edmonton Bulletin 51, 60 p.

Hamilton, W.B., 1969, Mesozoic California and the underflow of Pacific mantle: Geological Society of America, Bulletin, v. 80, p. 2409–2430.

Hamilton, W.B. and Myers, W.B., 1967, The Nature of Batholiths; U.S. Geological Survey Professional Paper 554-C, 30 p.

Hawkesworth, C. J., Turner, S. P., Gallagher, K., Hunter, A. G., Bradshaw, T. K. & Rogers, N. W. (1995). Calc-alkaline magmatism, lithospheric thinning and extension in the Basin and Range. Journal of Geophysical Research, v. 100, 10271–10286.

Hildebrand, R.S., and Whalen, J.B., 2015. Arc and slab-failure magmatism in Cordilleran batholiths II – The Cretaceous Peninsular Ranges batholith of Southern and Baja California: Paul Hoffman Volume, Geoscience Canada, v. 41, p. 399-458.

Hildebrand, R.S. and Whalen, J.B., 2017, The tectonic setting and origin of Cretaceous batholiths within the North American Cordillera: The case for slab failure magmatism and its significance for crustal growth. Geological Society of America Special Paper 532, 113 p..

Hildreth,W., and Moorbath, S., 1988. Crustal contributions to arc magmatism in the Andes of Central Chile; Contributions to Mineralogy and Petrology, v. 98, p. 455–489.

Hinchey, A.M., Davis, W.J., Ryan, J.J., and Nadeau, L., 2011. Neoarchean high-potassium granites of the Boothia mainland area, Rae domain, Churchill province: U-Pb zircon and Sm-Nd whole rock isotopic constraints; Canadian Journal of Earth Sciences, v. 48, p. 247-279.

Hoffman, P.F., 1988. United plates of America, the birth of a craton: Early Proterozoic assembly and growth of Laurentia; Annual Reviews of Earth and Planetary Science, v. 16, p. 543–603.

Hoffman, P.F. and Hall, L., 1993. Geology, Slave Craton and environs, District of Mackenzie, Northwest Territories; Geological Survey of Canada, Open File 2559, 1 sheet; 1 CD-ROM. doi:10.4095/183951

Jensen, L.S. A. 1976, A new cation plot for classifying subalkalic volcanic rocks; Ontario Division of Mines, MP66, 22p.

Le Maitre, R.W., 1989. A Classification of Igneous Rocks and Glossary of Terms; Oxford,

Blackwell, 193 p.

Lucas, S.B., Stern, R.A., and Syme, E.C., 1996. Flin Flon greenstone belt: Intraoceanic tectonics and the development of continental crust (1.92–1.84 Ga); Geological Society of America, v. 108, p. 602–629.

Maniar, P.D. and Piccoli, P.M., 1989. Tectonic discrimination of granitoids; Geological Society of America, Bulletin, v. 101, p. 635-643.

Martin, H., 1994. The Archean grey gneisses and the genesis of the continental crust; *in* The Archean Crustal Evolution: Developments in Precambrian Geology, (ed.) K.C. Condie; Elsevier, Amsterdam, p. 205-259.

McCurdy, M.W., Berman, R.G., Kerr, D.E., and Vaive, J.E., 2013. Geochemical, Mineralogical and Kimberlite Indicator Mineral Data for Silts, Heavy Mineral Concentrates and Waters, Duggan Lake Area, Nunavut (NTS 76H and 76I South); Geological Survey of Canada, Open File 7471, 22p.

McDonough, M.R., McNicoll, V.J., Schetselaar, E.M., and Grover, W., 2000. Geochronological and kinematic constraints on crustal shortening and escape in a two-sided oblique-slip collisional and magmatic orogen, Paleoproterozoic Taltson magmatic zone, northeastern Alberta; Canadian Journal of Earth Sciences, v. 37, p. 1549–1573.

McNicoll, V.J., Theriault, R.J., and McDonough, M.R., 2000. Taltson basement gneissic rocks: U-Pb and Nd isotopic constraints on the basement to the Paleoproterozoic Taltson magmatic zone, northeastern Alberta; Canadian Journal of Earth Sciences, v. 37, p. 1575-1596.

Mitchell, R.K., Berman, R.G., Davis, W.J., and Carr, S., 2017. Paleoproterozoic Metamorphism of the Thelon Tectonic Zone and margins of the Slave and Rae Archean cratons - insights into the nature and timing of the Slave-Rae Collision; Geol. Ass. Can. Prog. Abst., v. 40, p. 265.

Moyen, J.-F., 2009, High Sr/Y and La/Yb ratios: The meaning of the “adakitic signature”: Lithos, v. 112, p. 556–574.

Natural Resources Canada, 2013. Geoscience Data Repository: Aeromagnetic Data. On-line data from http://gdrdap.agg.nrcan.gc.ca/geodap/index_e.html.

Patino Douce, A.E. and Johnston, A.D., 1991. Phase equilibria and melt productivity in the pelitic system; implications for the origin of peraluminous granitoids and aluminous granulites; Contributions to Mineralogy and Petrology, v. 107, p. 202-218.

Pearce, J.A., 1996. Sources and settings of granitic rocks; Episodes, v. 19, p. 120-125.

Pearce, J.A., Harris, N.B.W., and Tindle, A.G., 1984, Trace element discrimination diagrams for the tectonic interpretation of granitic rocks; Journal of Petrology, v. 25, p. 956-983.

Peccerillo, A. and Taylor, S.R., 1976. Geochemistry of the Eocene calc-alkaline volcanic rocks from Kastamonu area, northern Turkey; Contributions to Mineralogy and Petrology, v. 58, p. 63-81.

Schultz, M.E.J., Chacko, T., Heaman, L.M., Sandeman, H.A., Simonetti, A., and Creaser, R.A., 2007. Queen Maud block: A newly recognized Paleoproterozoic (2.4-2.5 Ga) terrane in

northwest Laurentia; Geology, v. 35, p. 707-710.

Schwindinger, M., and Weinberg, R.F., 2017. A felsic MASH zone of crustal magmas -Feedback between granite magma intrusion and in situ crustal anatexis; Lithos, v. 284–285, p.109–121.

Shand, S.J., 1943. Eruptive rocks, their genesis, composition, classification, and their relation to ore deposits: Revised, 2d ed., John Wiley & Sons, New York, 444 p.

Streckeisen, A.L. and LeMaitre, R.W., 1979. Chemical approximation to modal QAPF classification of the igneous rocks; Neus Jahrbuch fur Mineralogie, v. 136, p. 169-206.

Sun, S.S. and McDonough, W.F., 1989. Chemical and isotopic systematics of oceanic basalts: implications for mantle composition and processes, *in* Magmatism in the Ocean Basins, (ed.) A.D. Saunders and M.J. Norry; Geological Society Special Publication, Blackwell Scientific, p. 313-345.

Swinden, H.S., Jenner, G.A., Kean, B.F., Evans, D.T.W., 1989. Volcanic rock geochemistry as a guide for massive sulphide exploration in central Newfoundland. In: Current Research, Newfoundland Dept. Energy and Mines, Geological Survey Report 89-1, 201-219.

Tarney, J. and Jones, C.E., 1994. Trace element geochemistry of orogenic igneous rocks and crustal growth models. Journal of the Geological Society, v. 151, p. 855-868.

Taylor, B.E., Berman, R.G., Whalen, J.B., Davis, W.J. (2017). Oxygen Isotope Reconnaissance Study of Magmatic Rocks in the Chantrey-Thelon area: GEM-2 Thelon Tectonic Zone. GAC-MAC Abstracts, v. 40, p. 372.

Tersmette, D., 2012. Geology, geochronology, thermobarometry, and tectonic evolution of the Queen Maud block, Churchill craton, Nunavut, Canada; unpublished M.Sc. thesis, Edmonton, Alberta, University of Alberta, 161 p.

Theriault, R.J., 1990. Evolution of the ca. 1.9 Ga Taltson magmatic zone, NWT: a Nd isotope perspective: M.Sc thesis, University of Ottawa, Ottawa, Ontario.

Theriault, R.J., 1992. Nd isotopic evolution of the Taltson magmatic zone, Northwest Territories, Canada: insights into early Proterozoic accretion along the western margin of the Churchill Province; Journal of Geology, v. 100, p. 465-475.

Thompson, P., 1986. Geology, Tinney Hills-Overby Lake (West Half), District of Mackenzie, Northwest Territories; Geological Survey of Canada, Open File 1316, Map, scale 1:125 000.

Thompson, P.H., 1989. An empirical model for metamorphic evolution of the Archaean Slave Province and adjacent Thelon tectonic zone, north-western Canadian Shield; *in* Evolution of metamorphic belts, (ed.) J.S. Daly, R.A. Cliff, and B.W.D. Yardley; Geological Society Special Publication 43, p. 245-263.

Vielzeuf, D. and Montel, J.M., 1994. Partial melting of metagreywackes; Part 1, Fluid-absent experiments and phase relationships; Contributions to Mineralogy and Petrology, v. 117, p. 375-393.

Wood, D.A., 1980. The application of a Th-Hf-Ta diagram to problems of tectonomagmatic classification and to establishing the nature of crustal contamination of basaltic lavas of

the British Tertiary volcanic province. Earth Planetary Science Letters. v. 50, p. 11-30.

Whalen, J.B. and Frost, C.D., 2013. The Q-ANOR diagram: A tool for the petrogenetic and tectonomagmatic characterization of granitic suites; South-Central Section, Geological Society of America, Austin, Texas, abstract.

Whalen, J.B., McNicoll, V.J., van Staal, C.R., Lissenberg, C.J., Longstaffe, F.J., Jenner, G.A., and van Breeman, O., 2006. Spatial, temporal and geochemical characteristics of Silurian collision-zone magmatism: an example of a rapidly evolving magmatic system related to slab break-off, Newfoundland Appalachians; Lithos, v.89, p.377-404.

Whalen, J.B., Pehrsson, S.J., and Rayner, N.M., 2016. Significance of pre-1860 Ma granitoid magmatism for crustal evolution and exploration targeting in the Flin Flon Assemblage, Trans-Hudson Orogen, Canada; Economic Geology, v.111, p.1021-1039.

White, A.J.R., and Chappell, B.W., 1983, Granitoid types and their distribution in the Lachlan Fold Belt, southeastern Australia. In: Roddick, J.A. (Ed.), Circum-Pacific Plutonic Terranes. Geological Society of America Memoir 159, p. 21-24.